



Large-scale integrated subglacial drainage around the former Keewatin Ice Divide, Canada reveals interaction between distributed and channelised systems

5 Emma L.M. Lewington¹, Stephen J. Livingstone¹, Chris D. Clark¹, Andrew J. Sole¹
and Robert D. Storrar²

¹ Department of Geography, University of Sheffield, Sheffield, UK

² Department of Natural and Built Environment, Sheffield Hallam University, Sheffield, UK

10

Abstract

We identify and map traces of subglacial meltwater drainage around the former
keewatin Ice Divide, Canada from ArcticDEM data. Meltwater tracks, tunnel valleys
15 and esker splays exhibit several key similarities, including width, spacing, their
association with eskers and transitions to and from different types, which together
suggest they form part of an integrated drainage signature. We collectively term these
features 'meltwater corridors' and propose a new model for their formation, based on
observations from contemporary ice masses, of pressure fluctuations surrounding a
20 central conduit. We suggest that eskers record the imprint of a central conduit and
meltwater corridors the interaction with the surrounding distributed drainage system.
The widespread aerial coverage of meltwater corridors (5-36 % of the bed) provides
constraints on the extent of basal uncoupling induced by basal water pressure
fluctuations and variations in spatial distribution and evolution of the subglacial
25 drainage system, which will modulate the ice dynamic response.

1. Introduction

30

Variations in the configuration of subglacial hydrological systems are key to
understanding some of the most dynamic ice sheet behaviour at a range of spatial and
temporal scales (e.g. Zwally et al., 2002; Das et al., 2008; Joughin et al., 2008; van de
35 Wal et al., 2008; Shepherd et al., 2009; Palmer et al., 2011; Fitzpatrick et al., 2013;
Doyle et al., 2014). Once water reaches the bed, its impact on ice flow is determined



by the hydraulic efficiency of the subglacial hydrological system. Theory developed at alpine glaciers suggests that increasing water pressure results in enhanced ice motion owing to reduced ice-bed contact (Lliboutry, 1968; Bindschadler, 1983) and where
40 sediment is present, enhanced sediment deformation (e.g. Engelhardt et al., 1978; Hodge, 1979; Iken and Bindshadler, 1986; Fowler, 1987; Iverson et al., 1999; Bingham et al., 2008). Water pressure at the bed depends on water supply to, storage within and discharge through the subglacial hydrological system (Iken et al., 1983; Kamb et al., 1985; Nienow et al., 1998). Hydraulically efficient drainage can accommodate and
45 evacuate greater meltwater flux with fewer and smaller spikes in basal water pressure, and thus has less impact on ice motion.



Traditionally the subglacial hydrological system has been conceptualised as a
binary model comprising (i) inefficient distributed drainage - taking the form of thin
50 films of water (Weertman, 1972), linked cavities (Lliboutry, 1986; Walder, 1986; Kamb, 1987), groundwater flow (Boulton et al., 1995) and / or wide shallow canals (Walder and Fowler, 1994); and (ii) efficient channelised drainage with conduits cut either up into the ice (Rothlisberger-channel) or down into the bed (Nye-channel) (e.g. Rothlisberger, 1972; Shreve, 1972; Nye, 1973; Hooke et al., 1990). While initially
55 proposed as independent elements, these two configurations are now thought to be frequently and extensively connected (e.g. Hubbard et al., 1995; Andrews et al., 2014).



In theory, in a steady-state system, water flows from surrounding high pressure distributed regions into lower pressure conduits. Borehole measurements of subglacial
60 water pressure, modelling and ice velocity proxy data (e.g. Hubbard et al., 1995; Gordon et al., 1998; Bartholomaeus et al., 2008; Werder et al., 2013; Tedstone et al., 2014) suggest, however, that given a sufficiently large and rapid spike in water delivery to a subglacial conduit, the hydraulic gradient can be reversed such that water is forced out and laterally away from the conduit across a zone some metres to several
65 kilometres wide that has been referred to as a Variable Pressure Axis (VPA) (Hubbard, 1995). Thus, during significant fluctuations in the delivery of surface water to the bed, conduits interact with their surroundings, supporting the notion of a three-system model of: channelised subglacial drainage connected to the supraglacial hydrological system; distributed subglacial drainage weakly connected to the subglacial channels;
70 and hydraulically isolated subglacial distributed drainage (Hoffman et al., 2016).



Despite these advances in understanding, observations of distributed and channelised drainage interactions are sparse, and so controls on their spatial distribution and temporal evolution remain poorly constrained.

75 1.1 Palaeo-meltwater landforms

Palaeo–meltwater landforms have been fundamental in inspiring and guiding conceptual and numerical models of how water self-organises into drainage systems beneath present day ice masses because they can be easily observed and investigated. Such landforms are therefore key to contextualising spatially and temporally limited contemporary observations and are commonly used to support and develop the theory of ice sheet hydrological systems (e.g. Shreve, 1985; Clark and Walder, 1994; Boulton et al., 2007a,b; 2009; Hewitt and Creyts, 2019). Much of this focus has been on landforms such as eskers, meltwater channels and tunnel valleys which indicate efficient channelised subglacial drainage (e.g. Shreve, 1985; Brennand, 1994, 2000; Clark and Walder, 1994; Punkari, 1997; Boulton et al., 2007a, b, 2009; Storrar et al., 2014a; Livingstone and Clark, 2016). We will now discuss each of these in more detail.



90 1.1.1 Eskers

Eskers are linear depositional landforms made up of glaciofluvial sand and gravel deposited from meltwater flowing through an ice mass in conduits metres to tens of metres in width and height. They exist as individual segments that often align to form networks extending up to several hundreds of kilometres (e.g. Shreve, 1985; Aylsworth and Shilts, 1989; Brennand, 2000; Storrar et al., 2014a; Stroeven et al., 2016) and are typically taken to record the former position and characteristics of Röthlisberger-channels (R-channels) thermally eroded into the base of the ice by turbulent water flow. While most studies reduce esker mapping to a single crest-line and consider the ‘classic’ single straight-to-sinuuous undulating ridge to be pervasive, more complex esker morphologies also occur (e.g. Banerjee and McDonald, 1975; Rust and Romanelli, 1975; Hebrand and Amark, 1989; Gorrell and Shaw, 1991; Warren and Ashley, 1994; Brennand, 2000; Mäkinen, 2003; Perkins et al., 2016; Storrar et al., 2019). These include fine-grained sandy fan shape elements or ‘splays’,



105 alongside and associated with the coarse gravelly central ridge (e.g. Cummings et al.,
2011a; Prowse, 2017). These splays are an order of magnitude wider and more gently
sloped than the main ridge (Cummings et al., 2011a). They are proposed to form in
both proglacial environments, representing subaqueous outwash fans deposited by
sediment laden plumes exiting a subglacial conduit into a proglacial lake (e.g. Powell,
110 1990; Hoyal et al., 2003; Cummings et al., 2011b), and / or subglacial environments,
with sedimentation in subglacial cavities alongside the main esker ridge during periods
of conduit **over-pressurisation** (e.g. Gorrell and Shaw, 1991; Brennand, 1994).



1.1.2 Meltwater channels and tunnel valleys

115

Erosional subglacial meltwater channels, or Nye-channels, incised into bedrock or
sediment substrate range in size from metres to tens of metres wide (e.g. Sissons,
1961; Glasser and Sambrook Smith, 1999; Piotrowski, 1999) to large tunnel valleys
several kilometres in width and tens of kilometres long (e.g. Kehew et al., 2012; van
120 der Vegt et al., 2012; Livingstone and Clark, 2016). Tunnel valleys are observed to
occur at various developmental stages from mature and clearly defined to indistinct
valleys often associated with hummocky terrain or as a series of aligned depressions
(e.g. Kehew et al., 1999; Sjogren et al., 2002). Their formation has been linked to
subglacial meltwater erosion at the ice-bed interface (c.f. Ó Cofaigh, 1996; Kehew et
125 al., 2012; van der Vegt et al., 2012) with the assumption that channels transported
large volumes of sediment and water. However, their precise mechanism of formation
is still debated with the main arguments focussing on i) catastrophic outburst formation
with rapid erosion following the release of sub or supraglacially stored water (e.g.
Piotrowski, 1994; Cutler et al., 2002; Hooke and Jennings, 2006; Jørgensen and
130 Sandersen, 2006) and ii) gradual steady-state formation with headward erosion of
soft-sediments in low water pressure conduits (e.g. Boulton and Hindmarsh, 1987;
Mooers, 1989; Praeg, 2003; Boulton et al., 2009).



Here, we use the term meltwater channel to refer to palaeo-evidence of erosional
135 channelised flow left on the ice sheet bed (i.e. the outline of the path the water took)
at all scales from N-channels through to tunnel valleys. **We use the term conduit to
refer to the active channelised flow beneath a contemporary ice mass (i.e. the
enclosed (sediment and / or ice walled) pipe carrying water at the ice-bed interface).**





1.1.3 Meltwater tracks

140

Detailed mapping in northern Canada and Scandinavia has identified the presence of linear tracks variously termed ‘hummock corridors’, ‘glaciofluvial corridors’, ‘washed zones’ and ‘esker corridors’, typically a few hundred meters to several kilometres wide and a few kilometres to hundreds of kilometres long (e.g. St-Onge, 1984; Dredge et al., 1985; Rampton, 2000; Utting et al., 2009; Burke et al., 2012; Kerr et al., 2014a, 2014b; Sharpe et al., 2017; Peterson et al., 2017; Peterson and Johnson, 2018; Lewington et al., 2019). These features often contain eskers and hummocks which vary in size, shape and relief (Peterson and Johnson, 2018) as well as ‘patches’ of glaciofluvial deposits and areas of exposed bedrock. While a subglacial meltwater origin is largely agreed upon, their precise mode of formation is not yet known. These features are collectively termed meltwater tracks hereon in.

145

150

Meltwater landforms are typically mapped and interpreted individually (e.g. Clark and Walder, 1994; Brennand, 2000; Storrar et al. 2013; Burke et al., 2015; Livingstone and Clark, 2016; Mäkinen et al., 2017) rather than as a holistic drainage signature (c.f. Storrar and Livingstone, 2017). As such, it is not yet clear whether or how differing expressions of subglacial drainage are interrelated and to what extent variations in drainage and / or background conditions (e.g. bed substrate, geology and local topography) control the preserved geomorphic signature we see today. This study aims to identify and map all discernible evidence of subglacial meltwater drainage across the Keewatin District of northern Canada from the ArcticDEM. We collectively refer to these as meltwater routes (MW_{Routes}). Producing an integrated map of all visible subglacial meltwater evidence allows us to report on the varying dimensions and geomorphological expressions of these features, to investigate associations between features traditionally treated separately and to explore potential controls on expression and formation.

155

160

165

2. Study Area

170

This study focusses on an area approximately 1 million km² to the west of Hudson Bay in northern Canada that surrounds the location of the former Keewatin Ice Divide (Fig. 1) (Lee et al., 1957; McMartin et al., 2004). The area generally exhibits low relief



and is underlain by resistant Precambrian bedrock that is either exposed or covered by till ranging from thin and discontinuous to thick and pervasive (e.g. Clark and Walder, 1994).

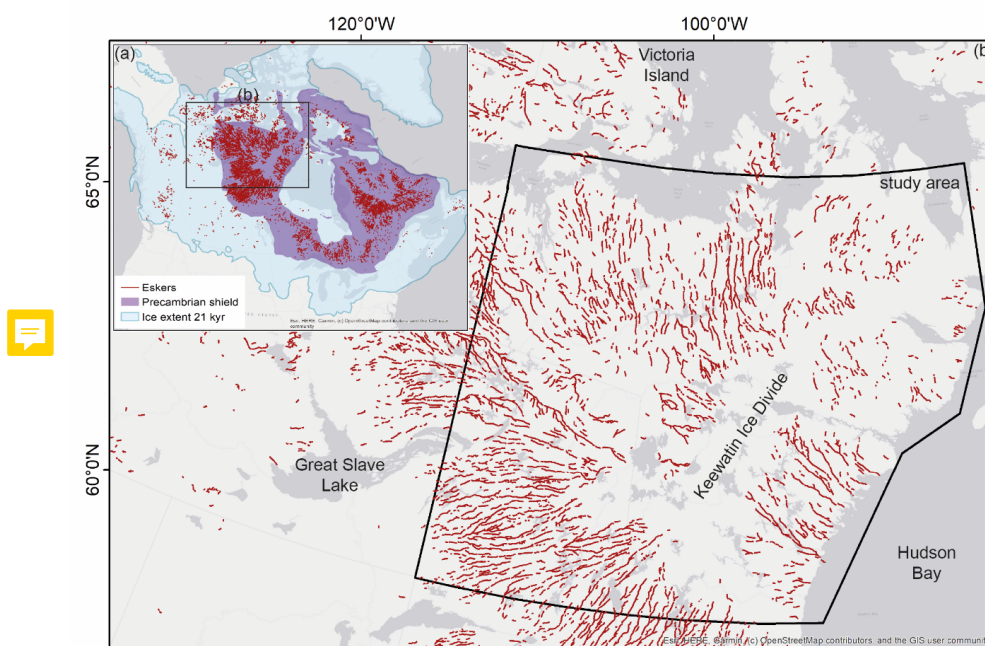


Figure 1. (a) Large-scale distribution of eskers around Hudson Bay (Storrar et al., 2013). The Laurentide Ice Sheet extent displayed in the inset is the Last Glacial Maximum (LGM) at 18 ¹⁴C ka BP (21.4 cal. ka BP) (Dyke et al., 2003) and the extent of the Precambrian shield is also mapped (Wheeler et al., 1996). (b) Zoomed in location of the study area focussed on the area around the former Keewatin Ice Divide.

Traditionally, eskers have been identified as the predominant meltwater landform within the Keewatin area, although meltwater tracks (MW_{Tracks}) (e.g. St-Onge, 1984; Aylsworth and Shilts, 1989; Rampton, 2000; Utting et al., 2009; Sharpe et al., 2017; Lewington et al., 2019) and meltwater channels (e.g. Storrar and Livingstone, 2017) have also been recorded. At a large scale, eskers radiate out from the ice divide, beneath which they are rare (Shilts et al., 1987; Aylsworth and Shilts, 1989; Storrar et al., 2013, 2014a). At a local to regional scale, they exhibit a dendritic pattern and 12–15 km quasi-uniform spacing (e.g. Banerjee and McDonald, 1975; St-Onge, 1984; Shilts et al., 1987; Bolduc, 1992; Storrar et al., 2014a).



105
Eskers have been widely mapped in northern Canada. Initial mapping was
largely undertaken by the Geological Survey of Canada using air photography and
field observations (e.g. Aylsworth and Shilts, 1989). This included mapping of 'esker
systems' - comprising a series of hummocks or short, flat-topped segments which
phase downstream into relatively continuous esker ridges or occasionally beaded
eskers - across 1.3 million km² of the Keewatin sector of the Laurentide Ice Sheet (LIS)
(Aylsworth and Shilts, 1989; Aylsworth et al., 2012). Discontinuous esker ridges are
connected to areas of outwash, meltwater channels or belts of bedrock stripped free
of drift. More recently, increasing availability of remotely sensed data allowed Storrar
et al., (2013) to digitise eskers at an ice sheet scale for the LIS (including the Keewatin
sector) using Landsat 7 ETM+ imagery. From this, a secondary dataset was derived
by interpolating a straight line between successive aligned esker ridges, creating a
continuous pathway, which reflects the location of the major conduits in which the
eskers formed (Storrar et al., 2014a).

3. Methods

3.1 Data sources and mapping

210
ArcticDEM 10 m resolution DEMs (freely available at
215 <https://www.pgc.umn.edu/data/arcticdem>), generated by applying stereo and auto-
correlation techniques to overlapping pairs of high-resolution optical satellite images
(Noh and Howat, 2015; Porter et al., 2018), were used in this study to identify and map
meltwater landforms. Eskers mapped by Storrar et al. (2013) from 30 m resolution
Landsat ETM+ multispectral imagery were used to inform further high-resolution esker
mapping from the 10 m resolution DEM. The automatic mapping approach developed
in Lewington et al. (2019) was used to create a first pass map of hummock corridors
– classified as meltwater tracks here (Appendices Fig. A1) to augment the improved
esker map. Together, these were used to create an integrated map of MW_{Routes} by
manually mapping centrelines of all visible traces of subglacial meltwater drainage
including meltwater tracks, meltwater channels and eskers. Multiple orthogonal
hillshades were generated to avoid azimuth bias (Smith and Clark, 2005) and mapping
was undertaken at a range of spatial scales to maximise the number of features
225 captured (Chandler et al., 2018).



3.2. Classification and morphometry

The MW_{Routes} were used to explore the occurrence and morphology of different
230 types of meltwater landforms. Former ice-margin estimates from Dyke et al. (2003)
were used as transects. These transects are spaced approximately 30–40 km apart
and in the study area, cover c. 1,000 years of deglaciation between 9.7 and 8.6 ka.
This period encompasses the final stages of deglaciation when the ice sheet was
experiencing a strongly negative surface mass balance with associated increasing
235 rates of meltwater production (e.g. Carlson et al., 2008, 2009). Retreat rates were
generally between 100–200 m yr⁻¹ from 13 to 9.5 ka, increasing rapidly between 9.5
and 9 ka to around 400 m yr⁻¹ after which retreat rate decreased briefly before another
increase from ~8.5 ka (Dyke et al., 2003).

240 When a MW_{Route} intersected a transect, an intersection point was added, and
the following information recorded:

- Landform type (i.e. esker ridge, esker with lateral splay, meltwater track or
meltwater channel)
- 245 - Width of landform (or landforms if an esker ridge was present within a meltwater
track, meltwater channel or surrounded by a lateral splay)
- Bed substrate and geology (Fulton, 1995; Wheeler et al., 1996).

Spacing between adjacent MW_{Route} centrelines was calculated along each transect
250 with centrelines at the end of each transect and those separated by clear breaks (e.g.
due to the coincidence of a lake) discounted. The total length of MW_{Route} centrelines
was calculated automatically in a GIS.

3.3 Testing controls on MW_{Routes} width and expression

255

This study takes a large-scale approach to exploring controls on MW_{Routes} width
and expression. While this approach results in a compromise in terms of data
resolution available for the surface substrate and geology maps, it also increases
statistical confidence in the results due to the larger sample size. Before analysis was



260 undertaken, three test sites were selected from the study area to allow for more
detailed mapping and comparisons (Appendices Figs. A2 and A3).

To explore substrate and geological controls on MW_{Route} occurrence,
distribution and properties, the overall length of MW_{Routes} overlying each substrate type
265 (Fulton, 1995) and geology (Wheeler et al., 1996) within the three test sites was
calculated. The total area of each basal unit within the test sites was also calculated
and values converted to percentages. Following this, the percentage area was
subtracted from the percentage of MW_{Routes} for each individual substrate and geology
type, giving a positive (over-represented) or negative (under-represented) value. Next,
270 MW_{Routes} were split and classified by feature expression (i.e. esker, esker with lateral
splay, glaciofluvial material, anabranching sections, meltwater channel and MW_{Track}).
The above analysis was repeated by feature type to explore whether
geomorphological expression is controlled by surface substrate / geology. It is
important to note that categorisations along MW_{Routes} were not always independent as
275 the same section was sometimes coded as a meltwater track and an esker with splay
/ glaciofluvial deposits as often 'positive' features are situated within wider erosional
corridors.

It was noted that landform type varies both across adjacent MW_{Routes} and along
280 individual MW_{Route} centrelines. To assess any potential relationship between landform
expression and background controls in more detail, individual centrelines were
selected and sampled with a higher frequency (5 km intervals). At each sample point
the width of the MW_{Track} / meltwater channel, the presence / absence of an esker (and
its width if present), surface substrate, bed geology and elevation were recorded.

285

To investigate the relationship between subglacial drainage and bed
roughness, the standard deviation of the ArcticDEM (resampled to 50 m) was
calculated using a 1 km and 5 km radius circular search window and this was
compared to the density of MW_{Routes} . Ice stream locations (Margold et al., 2015) were
290 also qualitatively compared to the distribution of MW_{Routes} .



4. Results

295 4.1 An integrated drainage signature

Mapping all traces of meltwater drainage reveals the ubiquity of former subglacial drainage across the study area (Fig 2). A total of 2,795 MW_{Routes} were mapped over a ~ 1 million km^2 area with a total length of 51,856 km. The MW_{Routes} exhibit a similar overall pattern to earlier esker maps (e.g. Aylsworth and Shilts, 1989; Storrar et al., 300 2013) radiating out from the former Keewatin Ice Divide. Greater than 90 % of mapped esker ridges in this region are estimated to occur along a MW_{Route} and therefore form part of this wider network of drainage features. In terms of the large-scale pattern, there are no obvious trends in MW_{Route} density, width or feature type 305 associated with margin retreat. However, the study area only covers approximately 1,000 years, associated with a period of intense meltwater production and rapid retreat.

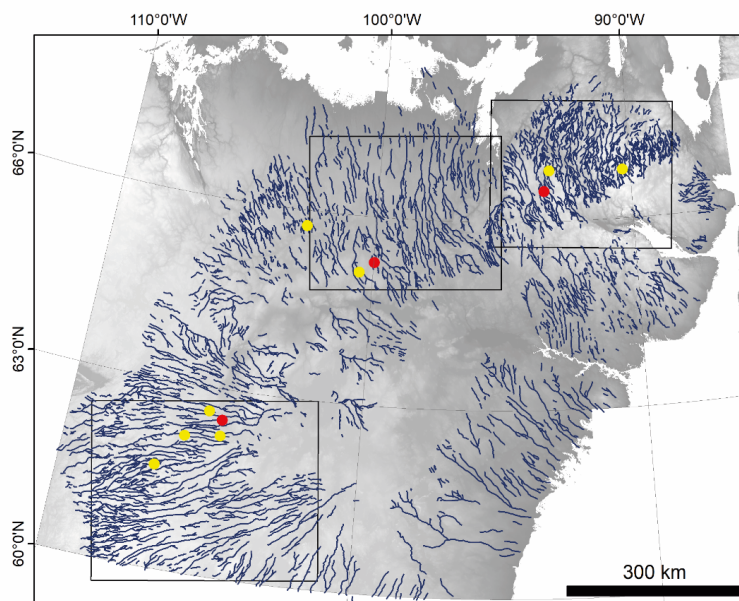


Figure 2. Integrated map of MW_{Routes} . Note how MW_{Routes} in this new map are less fragmented and denser than the existing esker map (Fig. 1b). Red points represent examples in Fig. 4 and yellow points those in Fig. 5. DEM created by Canadian Digital Elevation Model (CDEM). Ottawa, ON: Natural Resources Canada [2015]. 310



Esker ridges are recorded at 43 % of all sample points. Where they do occur, 87 % of them are flanked by a wider meltwater track, channel or splay. Comparing the updated esker map to the new MW_{Routes} map presented here confirms the large-scale association between eskers and wider meltwater features which often flank and / or connect intervening segments (Fig. 3). A wider meltwater feature in the scale of 100s-1000s m was recorded at 90 % of sample points (the remaining 6 % captured an esker ridge alone and 4 % were considered ambiguous and therefore not classified). This suggests that the mapping of complete MW_{Routes} creates a more complete and less fragmented drainage map with a higher number of tributaries and greater overall density, particularly in the Nunavut area (Fig. 3c). Nonetheless, evidence of palaeo-drainage remains noticeably absent beneath the location of the former ice divide (Fig. 2).

325

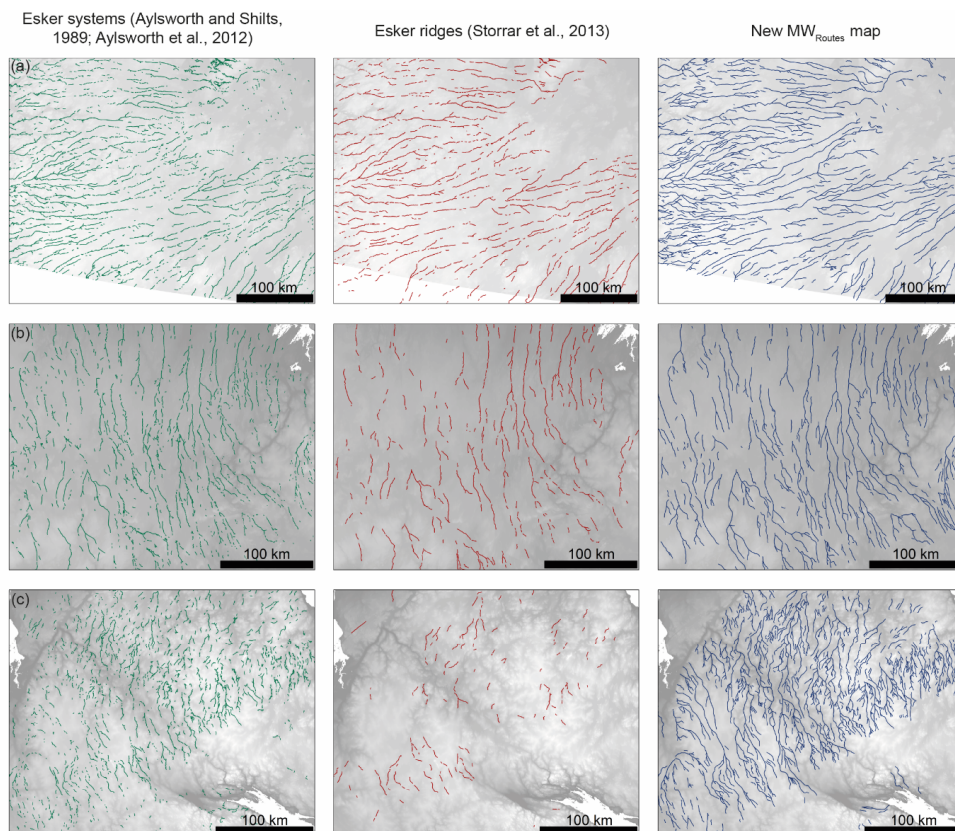
Table 1. Summary statistics for MW_{Routes} in the study area.

	Length (km)	Width (km)	Spacing (km)
Min	0.7	0.05	0.4
LQuartile	4.9	0.5	3.3
UQuartile	20.7	1.1	10.1
Max	339.9	3.3	77.9
Mean	18.5	0.9	8.1
Std dev.	26.9	0.6	7.4

MW_{Routes} reach a maximum of 340 km in length and 3.3 km in width (Table 1), but are noted to reach up to 760 km when they extend beyond the limits of the study area (Storarr et al., 2014a). Meltwater channels and meltwater tracks are typically an order of magnitude wider (mean width: 900 m) than the eskers which they often contain (mean width: 97 m). MW_{Routes} appear to vary in width around the ice sheet and along individual centrelines but show no clear (temporal) trend from the ice divide towards the margin. Within the study area, adjacent centrelines are spaced on average 8 km apart (Table 1). This is at the lower end of the range that has been observed and modelled (e.g. Banerjee and McDonald, 1975; St-Onge, 1984; Shilts et al., 1987; Hebrand and Amark, 1989; Bolduc, 1992; Boulton et al., 2009; Hewitt, 2011). Like variations in width, there appears to be no coherent change in spacing over time within this area (Fig. 3).



4.2 Comparison to previous regional – large scale mapping



345 **Figure 3.** Comparison of existing mapping of 'esker systems' (green) from air photo
interpretation (Aylsworth and Shilts, 1989; Aylsworth et al., 2012), esker ridges (red) from
Landsat imagery (Storrar et al., 2013) and the new MW_{Routes} from the ArcticDEM (blue).
Mapping of MW_{Routes} includes all traces of subglacial meltwater flow i.e. eskers, eskers with
lateral splay, meltwater tracks and meltwater channels. The locations of (a) (test site 1), (b)
350 (test site 2) and (c) (test site 3) are identified in Fig. 2. DEM(s) created from the Canadian
Digital Elevation Model (CDEM). Ottawa, ON: Natural Resources Canada. [2015]

This paper extends earlier work which recognises links between eskers and
355 broader traces of subglacial meltwater flow but does not explicitly describe or formally

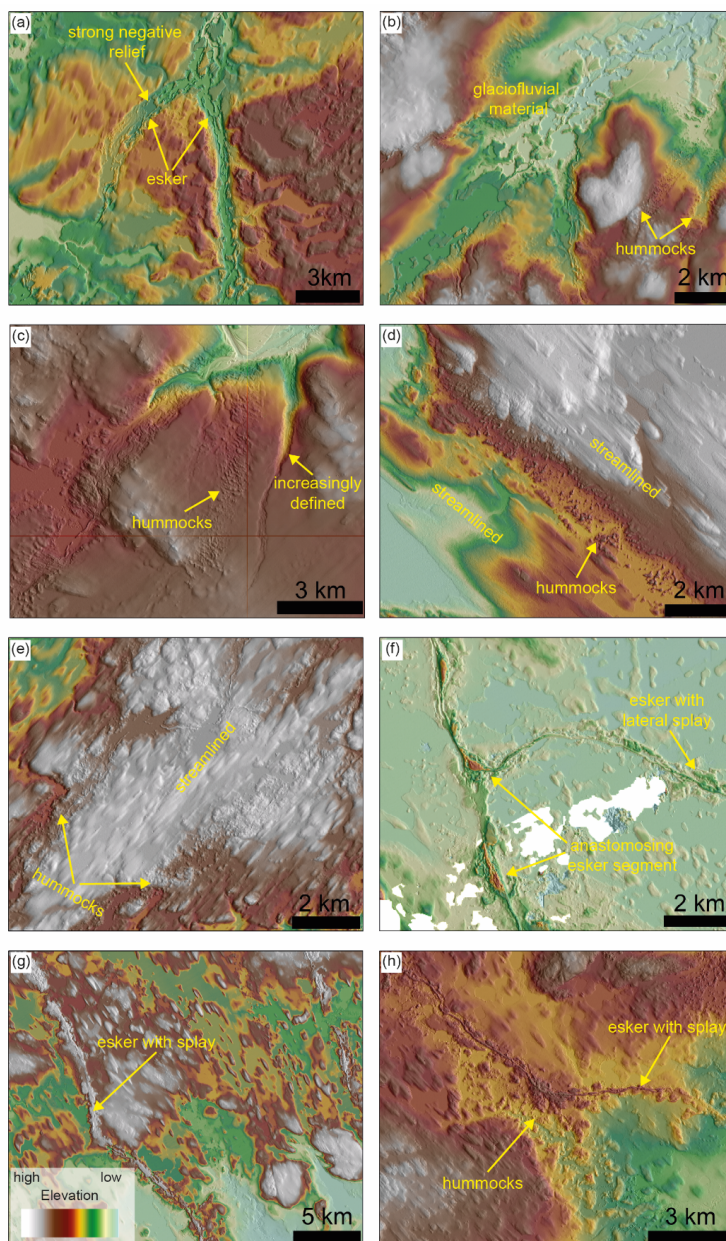


quantify them (e.g. Aylsworth and Shilts, 1989; Storrar et al., 2014a). It is encouraging that despite different datasets and mapping procedures, the overall patterns are similar (Fig. 3). Here we go beyond mapping eskers alone and identify and classify each part of the MW_{Routes} , including those which do not contain an esker. We describe them in detail (section 4.3) and explore the role of background controls in influencing geomorphic expression (section 4.4), providing insight into the drainage system operation (section 5).

4.3 Geomorphological variations

365

Landforms along MW_{Routes} exhibit a high degree of geomorphic variability in terms of relief and definition (Fig. 4). Some exhibit strongly negative relief (down to ~30 m below their immediate surroundings) and distinct boundaries, i.e. meltwater channels (Fig. 4a and 4c), while others exhibit negligible relief and are more difficult to differentiate from their surroundings i.e. meltwater tracks (e.g. Fig. 4d and 4e) or even exhibit positive relief i.e. eskers with lateral splay (e.g. Fig. 4f, 4g and 4h). Channel edges vary from straight to crenulated and from continuous to discontinuous. A variety of forms are found within the meltwater tracks and meltwater channels. These include hummocks of varying size, shape and relief and eskers and associated glaciofluvial material (e.g. Fig. 4e and 4f). In places, till may be entirely eroded revealing patches of bedrock. Eskers display a higher degree of variability along the MW_{Routes} with single, continuous straight-to-sinuuous ridges the exception rather than the norm (e.g. Fig. 4a and 4b).



380

Figure 4. Different geomorphological expressions observed along MW_{routes} in the Keewatin sector of the Laurentide Ice Sheet: (a-c) negative relief features with hummocks, eskers and glaciofluvial material within. They also demonstrate how features can vary in expression over short distances. (d-e) moderate to negligible relief features, defined by the presence of hummocks which stand out from the surrounding streamlined terrain. (f) two MW_{Routes} with

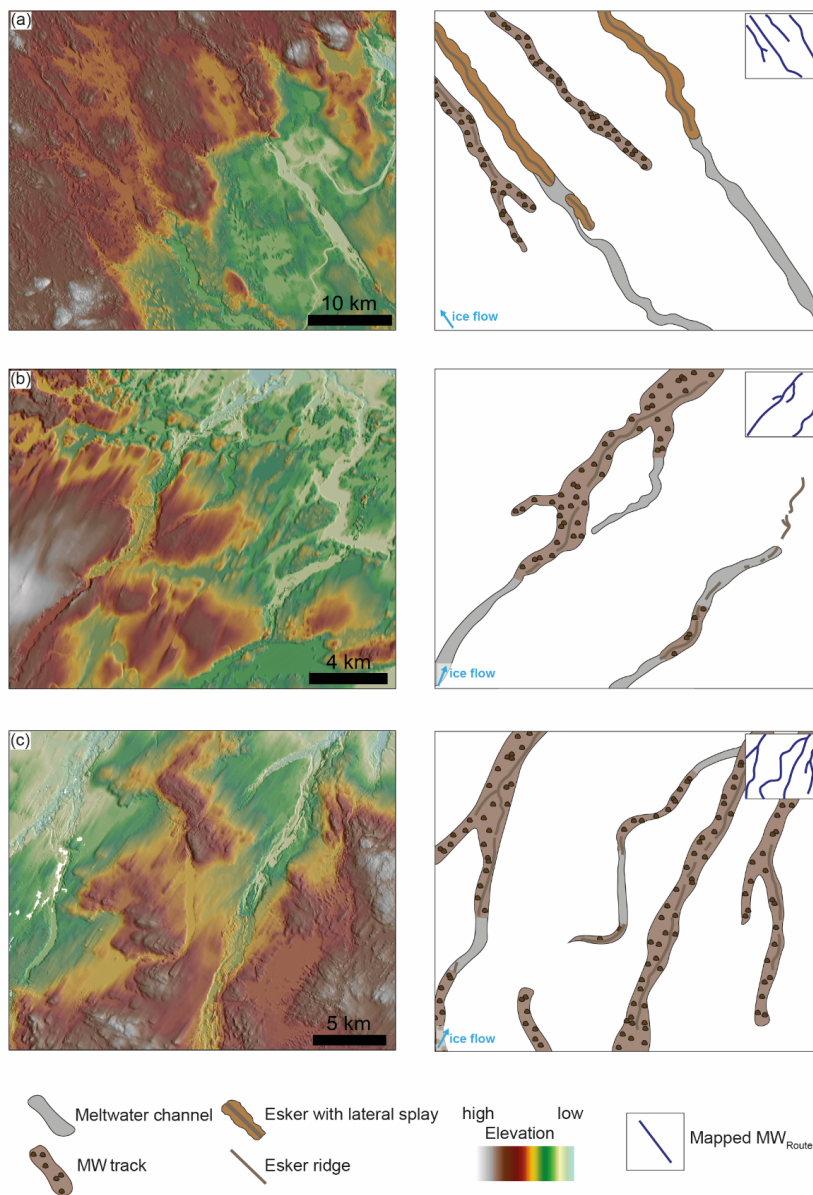
385



multiple sections of anastomosing eskers which join into a single feature downstream. (g) lateral splay surrounding a central esker ridge. (h) esker with splay joining a MW_{Track} from the SE perhaps indicating multiple stages of flow. DEM(s) created by the Polar Geospatial Center from DigitalGlobe, Inc. imagery.

390

Geomorphological expression varies both across flow (i.e. between adjacent centrelines) and along flow (i.e. along individual centrelines). Variations in landforms are recorded along individual MW_{Routes} by multiple transitions to and from landform classifications. Figure 5 shows examples of downstream transitions from meltwater channels to eskers with lateral splay (e.g. Fig 5a) and from meltwater channels to meltwater tracks and back (e.g. Fig. 5b and 5c).



400 **Figure 5.** Examples of transitions and associations along MW_{Routes} . The left panel shows the
 DEM and the right panel shows an interpretation of the feature types with an inset (top right)
 showing how MW_{Routes} are mapped as single lines through all types. White patches in the DEM
 represent areas of missing data due to the presence of hydrological features (e.g. lakes and
 rivers) and / or in areas of cloud cover and shadow. DEM(s) created by the Polar Geospatial
 405 Center from DigitalGlobe, Inc. imagery.



Despite variations in expression (e.g. relief, definition and the presence or absence of hummocks, glaciofluvial material and/ or eskers), meltwater tracks, meltwater channels and eskers with lateral splays are all associated with eskers (Fig. 4) and form an integrated and coherent large-scale spatial pattern (Fig. 5).
410 Furthermore, they display a qualitatively similar width range - several hundred meters to ~3 kilometres (Fig. 6) – although, the null hypothesis that the data in each pairing are from the same continuous distribution using the two-sample Kolmogorov-Smirnov test could not be rejected for any pairings (esker, esker with splay, meltwater channel and meltwater track) at the 5 % significance level.

415

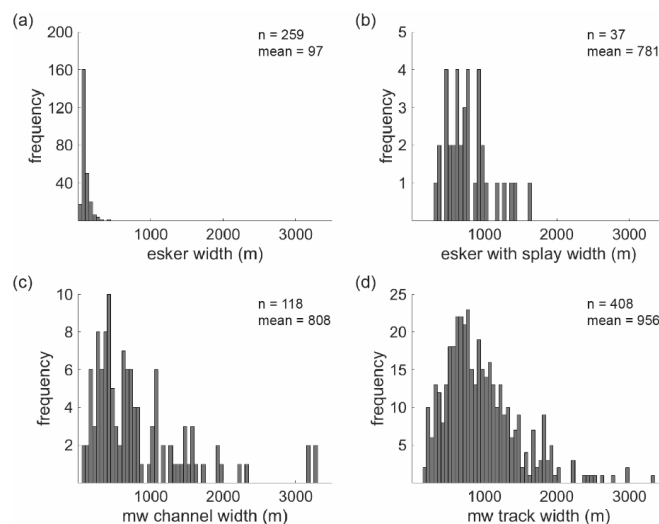


Figure 6. Width distributions (in metres) of (a) esker ridges, (b) eskers with lateral splay, (c) meltwater channels and (d) meltwater tracks. Note the similarity in distributions between eskers with lateral splay, meltwater channels and meltwater tracks.
420

4.4 Controls on the width and expression of meltwater landforms

425 Most subglacial meltwater landforms occur within areas of till (Fig. 7). Meltwater tracks, eskers with lateral splays and meltwater channels are all overrepresented in areas of till blanket, while esker ridges are strongly underrepresented. Meltwater



features appear most commonly over areas of metamorphic bedrock, although meltwater channels (incisional features) are overrepresented on more erodible
 430 sedimentary rocks.

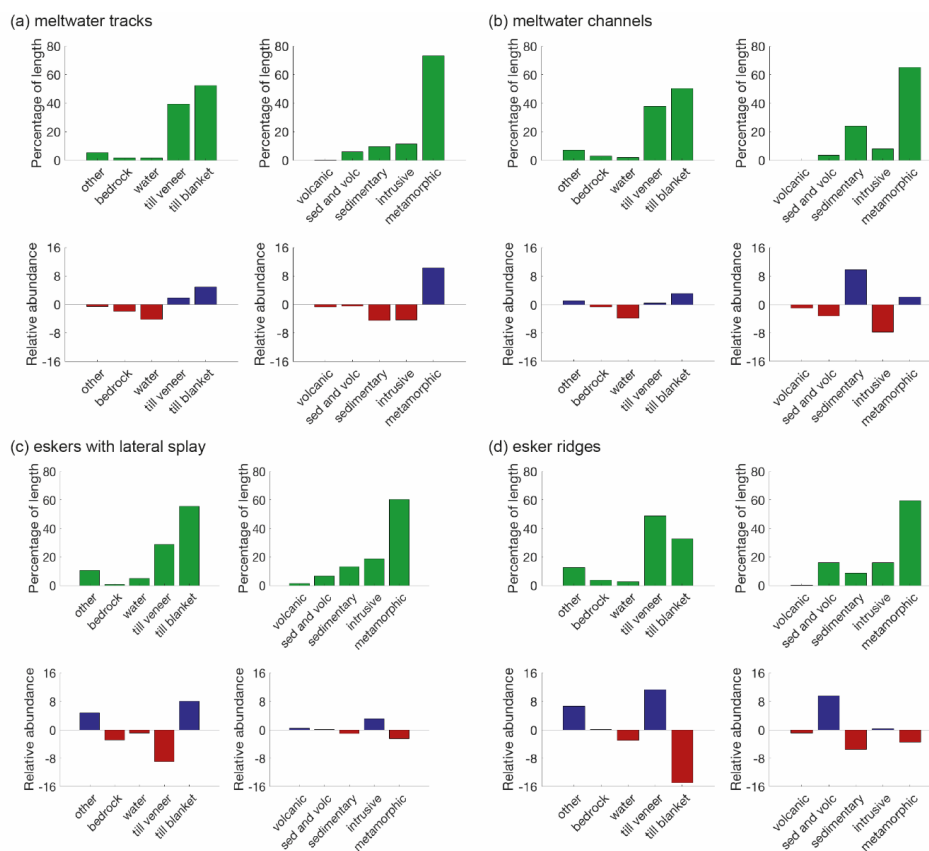


Figure 7. Substrate control on geomorphological expression. Occurrence (percentage of length) and relative abundance of different meltwater features over varying surface substrates
 435 (Fulton, 1995) and background geology (Wheeler et al., 1996). ‘Other’ includes marine, lacustrine and glaciofluvial sediments.

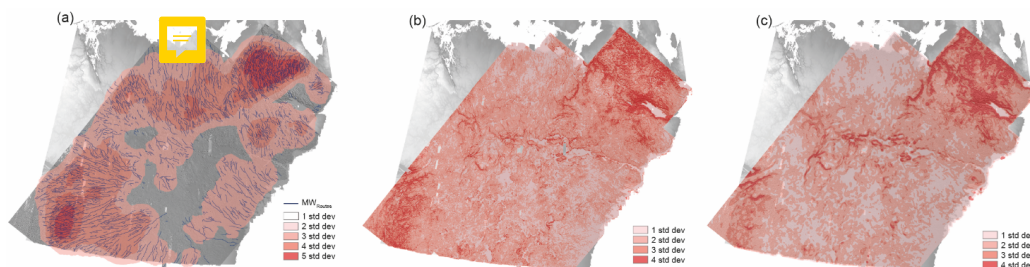
Figure 8 reveals two areas with a high density of MW_{Routes} – the largest in the NE
 440 and the other in the SW. These coincide qualitatively with areas of high local topographic variation (i.e. high standard deviation) at both scales of roughness



calculation (1 km and 5 km). Palaeo-ice streams are rare in the Keewatin District region (Stokes and Clark, 2003a,b; Margold et al., 2018), but where they do occur (e.g. Dubawnt Lake and Maguse ice streams), MW_{Routes} are noticeably sparser and

445

more fragmented (Fig. 9). On the bed of the Dubawnt Lake Ice Stream, the MW_{Routes} also exhibit a more dendritic arrangement and extend further towards the ice divide.



450 **Figure 8.** Density of MW_{Routes} (a) compared to local bed roughness (standard deviation) using (b) 1 km and (c) 5 km search window where darker colours represent greater deviation from the mean. DEM(s) created by the Polar Geospatial Center from DigitalGlobe, Inc. imagery and the Canadian Digital Elevation Model (CDEM). Ottawa, ON: Natural Resources Canada. [2015].

455

To explore potential controls governing how meltwater landform expression varies with changing background conditions, detailed measurements of width, feature type and substrate were extracted along individual MW_{Routes} (Fig. 10). Although there is no consistent ratio between esker width and the associated meltwater track / meltwater channel width at sample points across the whole study area, qualitatively there is a positive relationship between the two, with both increasing and decreasing in phase (Fig. 10). Esker width varies along individual pathways (varying by almost 300 % (Fig. 10b)) and expressions range from a single well-defined ridge to multiple, fragmented and anabranching sections. The MW_{Route} in Fig. 10b suggests that wider sections broadly coincide with higher bed elevations and the presence of more deeply eroded, yet narrower sections with decreasing elevation. In Fig. 10d we observe a large increase in width associated with a rapid increase in elevation, which also coincides with a transition from a strongly negative feature (a meltwater channel) to a positive /

465



470 depositional feature (esker with lateral splay). This sharp transition is related to the
emergence of the MW_{Route} out of the Thelon sedimentary basin.

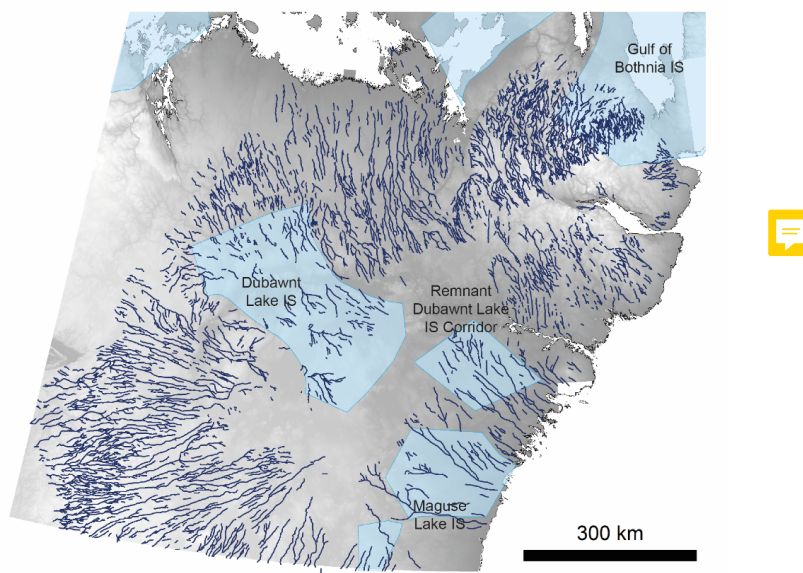
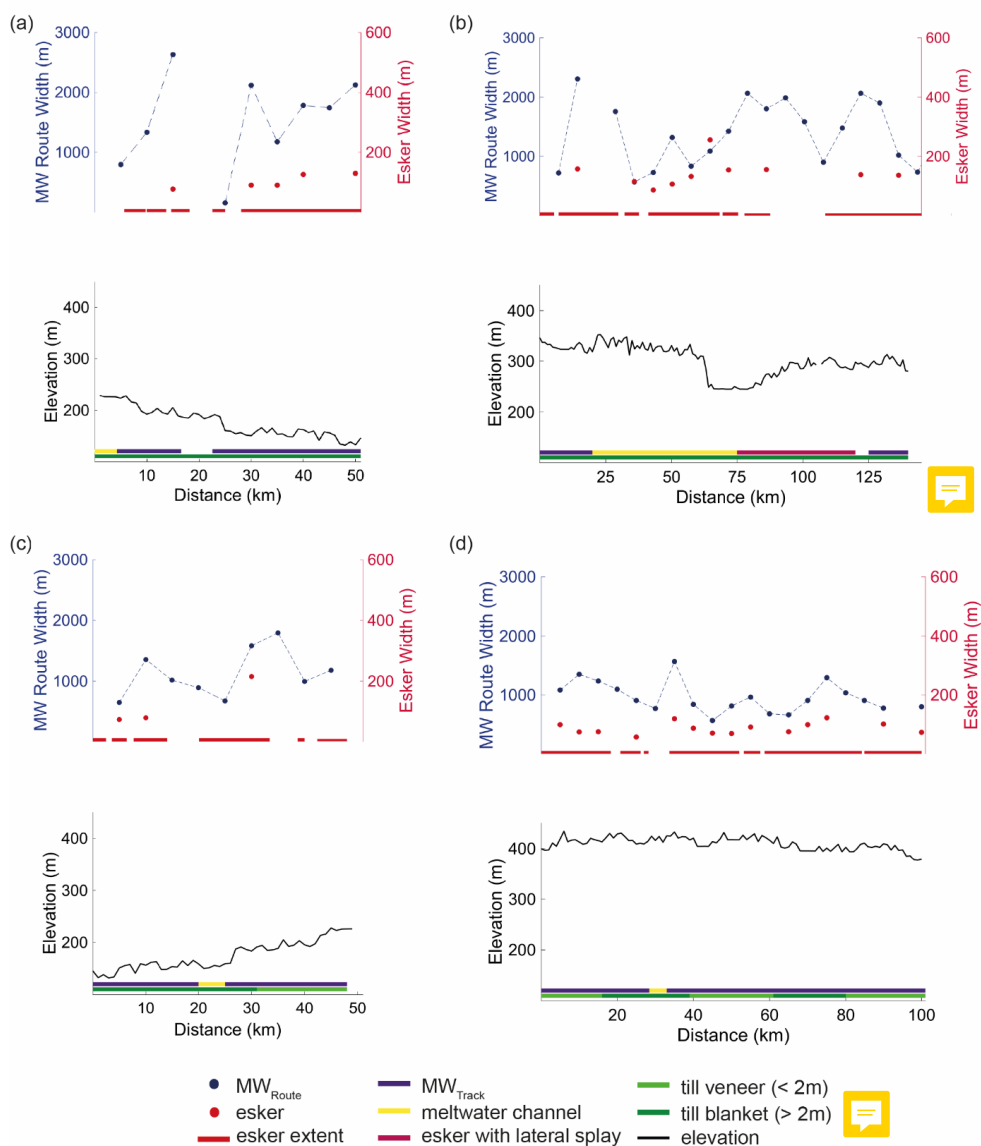


Figure 9. Comparison of MW_{Routes} and palaeo-ice streams (Margold et al., 2015). Note that
the few palaeo-ice streams that do occur within our study area tend to be associated with
475 fewer MW_{Routes} . MW_{Routes} on the bed of the Dubawnt Lake Palaeo-Ice Stream are also
distinctively more dendritic. DEM(s) created the Canadian Digital Elevation Model (CDEM).
Ottawa, ON: Natural Resources Canada. [2015].

480

485



490

Figure 10. Exploring local-scale controls on MW_{Route} width and expressions. Detailed profiles (sampled at 5 km intervals along individual MW_{Routes}) show how esker extent, elevation, feature expression and surface substrate vary along flow from the interior (left) to the exterior (right).

495



5. Discussion

Our new MW_{Routes} map shows that meltwater tracks, meltwater channels and esker
500 splays which flank and connect (in an along-flow direction) esker ridges are a dominant
part of the landscape across the former Keewatin sector of the LIS. Mapping complete
drainage pathways means we are better able to identify regional meltwater drainage
patterns and unravel controls on feature expression.

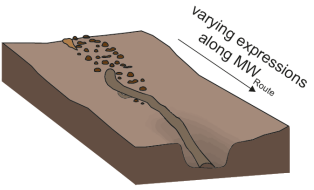
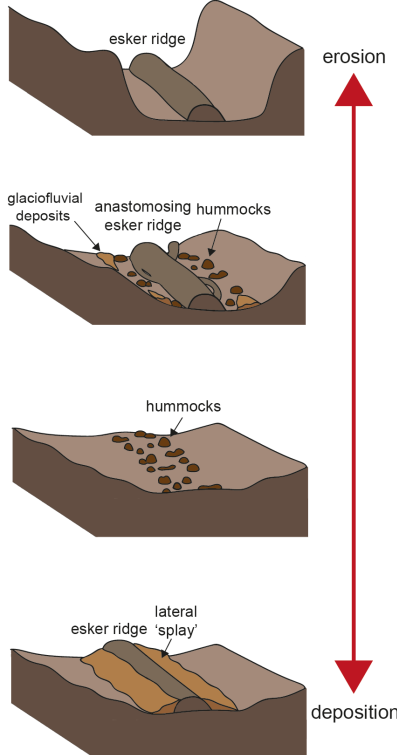

505 The large-scale distribution and pattern of meltwater tracks, channels and
eskers with lateral splays exhibit several key similarities, including their width, spacing,
association with eskers and occurrence within an integrated network characterised by
transitions to and from different types along individual MW_{Routes} (Figs. 4-6). Together,
this provides strong evidence that these meltwater landforms are varying expressions
510 of the same phenomenon and we therefore collectively group these features with
widths in the order of 100s to 1000s of meters and term them meltwater corridors
($MW_{Corridors}$) (Table 2). This is consistent with previous conceptual work linking
meltwater landforms. For example, Sjogren et al., (2002) identify various expressions
of tunnel valley (meltwater channel) that they attribute to different developmental
515 stages, from discontinuous through to fully developed valleys. Peterson and Johnson
(2018) suggest that negative relief hummock corridors (meltwater tracks) are a type of
tunnel valley and positive relief hummock corridors are the same as features
previously identified and termed 'glaciofluvial corridors' in Canada (e.g. Utting et al.,
2009).

520

525



530 **Table 2.** Proposed classification for subglacial meltwater traces observed on palaeo-beds. MW_{Routes} encompasses all evidence and consists of $MW_{Corridors}$ i.e. all traces which exhibit a width in the order 100's of meters (negative and positive relief) and esker ridges (width in the order of 10's of meters).

Proposed Classification	Description	Example
MW_{Route}	All traces of subglacial meltwater drainage (i.e. all of below)	
$MW_{Corridor}$	<p><i>'Negative':</i></p> <ul style="list-style-type: none"> - Meltwater Channel: <ul style="list-style-type: none"> - Tunnel channel - Tunnel valley - Hummock corridor (negative) (e.g. Peterson and Johnson, 2018; Lewington et al., 2019) - Erosional corridor (e.g. Burke et al., 2011) - Esker corridor (e.g. Sharpe et al., 2017) <p><i>'Positive':</i></p> <ul style="list-style-type: none"> - Meltwater corridor (e.g. Rampton, 2000) - Washed zone (e.g. Ward et al., 1997) - Glaciofluvial corridor (e.g. St-Onge, 1984; Utting et al., 2009) - Hummock corridor (positive) (e.g. Peterson and Johnson, 2018; Lewington et al., 2019) - Esker with splay (e.g. Cummings et al., 2011) 	
Esker ridge	Single esker ridge	



535 While recognised previously in local case studies (e.g. St-Onge, 1984; Rampton,
2000; Utting et al., 2009), we confirm that across this 1 million km² area of the former
LIS, MW_{Corridors} of varying geomorphic expression are widespread rather than an
isolated phenomenon. Within the study area, 87 % of all esker ridges were flanked by
a MW_{Corridor}. Esker ridges alone were captured at just 6 % of our sample points while
540 a MW_{Corridor} was recorded at 90 % (7 % of these were lateral splay, 21 % were
meltwater channels and 73 % were meltwater tracks) - the remaining 4 % were coded
as unclassified. However, we do note that the presence / absence of an esker at the
sample point may not be indicative of the entire length of the MW_{Route} as in many cases
the esker ridge within a MW_{Corridor} was fragmented. This suggests that the model of R-
545 channels across the Canadian Shield (e.g. Clark and Walder, 1994) is an
oversimplification and the range of landforms observed suggests the presence of
various modes of subglacial drainage varying between R-channels entirely cut up into
the ice to those incised into the bed with a range in-between. Variations in form and
pattern are likely to have been influenced by glaciological conditions, including ice
550 velocity, viscosity, temperature, and thickness, hydraulic potential gradient and water
flux, and background conditions such as basal substrate, topography and local scale
roughness.

555 **5.1 A proposed model of formation: interaction of channelised and distributed drainage elements**

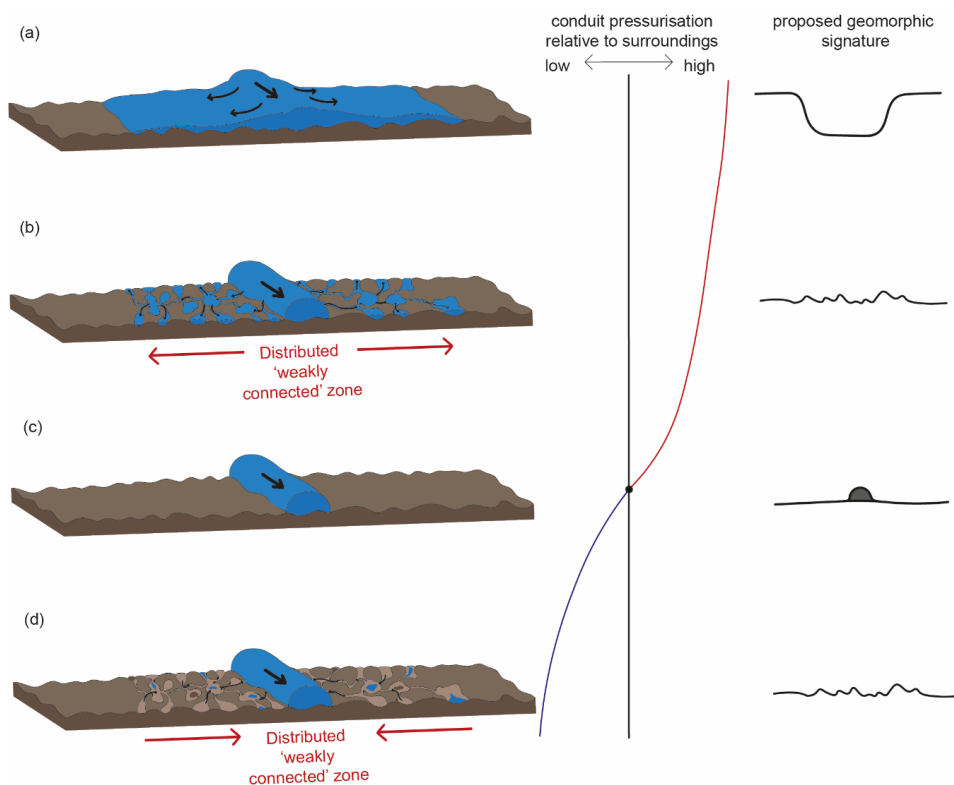
To interpret palaeo-landforms and reconstruct subglacial meltwater behaviour
an understanding of the processes that formed the landforms is needed (i.e. the
'glacial inversion' problem, e.g. Kleman and Borgström, 1996). One approach to
560 understanding glacial processes is through contemporary observations. In this
section, we demonstrate how modern observations and modelling of the Variable
Pressure Axis (VPA) around a subglacial conduit (e.g. Hubbard et al., 1995) is
consistent with the form and distribution of mapped MW_{Corridors} and can explain the
range of depositional to erosional signatures observed in the study area.

565

In steady-state conditions, conduits theoretically operate at a lower pressure
than the surrounding high-pressure weakly connected system, and therefore will
typically draw water in from their surroundings. However, variations in borehole water



570 pressure measurements observed beneath glaciers in the Alps (e.g. Hubbard et al.,
1995; Gordon et al., 1996) and Alaska (e.g. Bartholomaus et al., 2008), ice velocity
575 measurements taken from the Greenland Ice Sheet (e.g. Tedstone et al., 2014) and
numerical modelling (e.g. Werder et al., 2013), suggest that large and ~~or~~ rapid
meltwater inputs can cause spikes in conduit water pressure (Cowton et al., 2013).
This temporarily reverses the hydraulic potential gradient and causes water to flow out
580 of the conduit and into the surrounding weakly-connected drainage system (Fig. 11).
This is because the conduit cross-sectional area cannot be expanded rapidly enough
by wall melt to accommodate high frequency (e.g. diurnal surface melt) and / or high
magnitude (e.g. supraglacial lake drainage) fluctuations in meltwater delivery. As
meltwater delivery to the conduit wanes or the conduit cross-sectional area grows at
585 a rate sufficient to accommodate the additional meltwater input, water pressure in the
conduit decreases and the conduit will again begin to capture water from its
surroundings. Hubbard et al., (1995) note that the pressure perturbation decreases
with lateral distance from the conduit like a dissipating wave across the VPA. The
distance either side of the conduit influenced by these variations (i.e. the width of the
VPA) appears variable over time and space, reaching a maximum of ~140 m in the
Alps (Hubbard et al., 1995; Gordon et al., 1996) and modelled to be ~2 km for the
western margin of the GrIS (Werder et al., 2013). This tallies well with the spectrum of
MW_{Corridor} widths observed in this study, which range from ~100 m to > 3 km.



590

Figure 11. The interaction between a central conduit and the surrounding distributed 'weakly connected' zone with direction of water flow into and out of the conduit dependent on the variability and magnitude of discharge (Q). Water is forced out of the central conduit into the surrounding distributed system during periods of high Q (a-b) likely resulting in net erosion – and water and sediment flow back into the conduit during periods of low Q (d) – resulting in erosion or deposition of hummocks. Eskers are thought to be deposited in the conduit near the ice margin during the final stages of deglaciation.

595

600

Here, we propose that $MW_{\text{Corridors}}$ are the geomorphic signature of a VPA and represent the interaction between a conduit and the surrounding weakly connected system. Variations in MW_{Corridor} expressions are hypothesised to occur due to variations in discharge and pressure (frequency, magnitude and duration) as well as



605 **background** glaciological, geological and topographical conditions, which together determine the relative geomorphic activity (i.e. net erosion or deposition).

In this model, erosion of corridors with negative relief on the order of metres to 10s of metres depth is likely the result of large magnitude perturbations such as supraglacial or subglacial lake drainages, with the rising limb of the flood event over-pressurising the conduit and flooding the entire VPA (Fig. 11a). Flooding of this broader VPA zone is analogous to a narrow sheet flood causing localised flotation or hydraulic lifting (e.g. Brennand, 1994); similar processes have been recorded during jökulhlaups in Iceland (e.g. Russell et al., 2007). Flow across the VPA would enhance erosion by mobilising and entraining unconsolidated sediment in the **high velocity flow** (e.g. Russell et al., 2006 and references within). As the flood event wanes, the pressure perturbation is reversed causing water **and sediment to flow back towards** the main conduit where it is rapidly evacuated. Less well defined features that have experienced up to a few metres of erosion (i.e. those with more subdued relief and less well defined boundaries) **may be the result of repeated lower magnitude drainage and pressure perturbations (e.g. from diurnal melt or rainfall) forcing water out across the VPA.** Instead of completely overwhelming and flooding the system, these events may just fill and expand adjacent cavities (Fig. 11b). **Delivery of water to the bed is likely to occur at approximately the same location with lakes and crevasses 'locked' into place by basal topography (e.g. Gudmundsson, 2003; Sergienko, 2013; Ignéczi et al., 2018),** resulting in repeated drainage down the same pathways. In this scenario, the width of $MW_{Corridors}$ may represent a single maximum flow event or may represent the lateral merging of multiple narrower flow events - as has been proposed for the formation of some tunnel valleys (e.g. Jørgensen and Sandersen, 2006; **Kehew et al., 2012**) – if the central conduit is positioned in a slightly different position across the bed over time.

Sedimentological investigations suggest that hummocks within meltwater tracks can occur as a result of erosion (e.g. Rampton, 2000) and / or deposition (e.g. Utting et al., 2009) and our proposed model is able to explain each of these. Repeated coupling / uncoupling of the ice-bed interface as water is forced in and out of the VPA (Cowton et al., 2012) and subsequent erosion over seasons or longer may explain the hummocky topography we see today (Fig. 4). **Depositional hummocks** may be formed



640 by a rapid increase in cross-sectional area associated with a breach in the conduit
margin (i.e. it becomes unsealed) and flow across the VPA, facilitating rapid deposition
within minor conduits and cavities (e.g. Brennand, 1994). When the conduit returns to
being hydraulically isolated from the VPA following a decrease in water flow and
pressure, standing bodies of water left within the cavities may also deposit minor fans
which build up over time (Brennand, 1994). Alternatively, sediment may be trapped
645 within cavities formed during turbulent sheet flow as water velocities subsequently
decrease (Utting et al., 2009). Indeed, it is possible that lateral splays associated with
esker ridges also formed due to conduit breaching and subsequent deposition, with
outward fining in lateral fans suggesting conduit unsealing and decreasing hydraulic
power (Cummings et al., 2011b). Finally, hummocks may be a combination of erosion
and deposition. This is not dissimilar to the interpretation of triangular shaped
650 landforms ('murtoos') which are thought to form from subglacial till transported by
creep which is then eroded and shaped by subglacial meltwater, and represents high
pressure distributed drainage within a 'weakly connected' zone upstream of
channelised drainage (Mäkinen et al., 2017; Ojala et al., 2019).

655 Previous research indicates that esker ridges can be superimposed on hummocks
within $MW_{Corridors}$ (e.g. Peterson et al., 2018), but to date, there are no examples of
hummocks overlying eskers. Esker ridges do not always sit at the centre of their
 $MW_{Corridor}$ but instead meander across them, and are recorded alternately as left,
central or right at different transect points. This is consistent with eskers being the final
660 depositional imprint of channelised drainage within the large-scale MW_{Routes} network,
with formation close to the ice margin (e.g. Hebrand and Amark, 1989; Storrar et al.,
2014b; Hewitt and Creyts, 2019; Livingstone et al., in review), while the corridors
represent a composite imprint of drainage over a longer period.

665

670



5.2 A brief comment on possible alternative models

While we support the proposed
675 model above, we acknowledge there are
alternative formational mechanisms that
can explain the wide meltwater tracks. In
particular, it is possible that the width of
meltwater tracks (i.e. an order of
680 magnitude greater than the eskers
commonly residing within them) is the
consequence of a migrating conduit at the
bed (Fig. 12). Within the study area,
eskers are recorded at various positions
685 across the meltwater tracks (i.e. not
always at the centre) and are alternatively
recorded as left or right aligned at various
points down flow. To the best of our
knowledge, there is no published research
690 on the migration of contemporary conduits
across ice sheet beds, although they may
be expected to respond to variations in
location or flow conditions by vertical and
horizontal movement in a manner
analogous to a central river within a
695 floodplain. Therefore, it is possible that the
meltwater corridor width is a result of a
migrating central conduit.

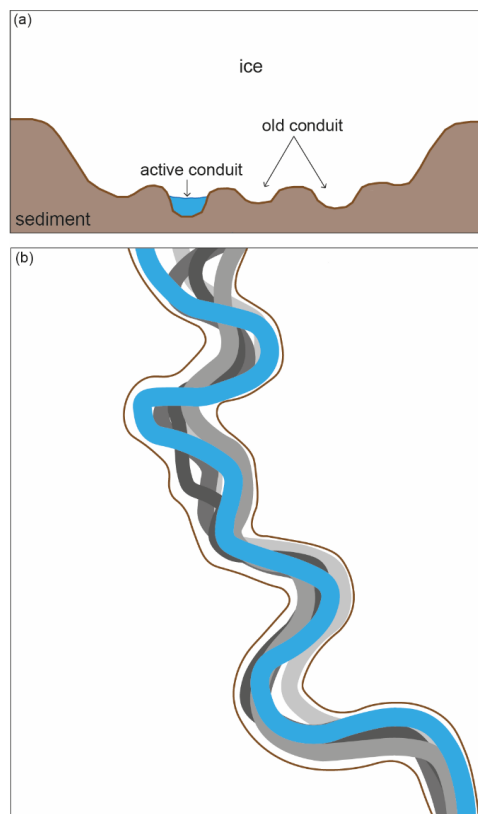


Figure 12. Schematic of alternative explanation of meltwater track width as a result of a migrating central conduit analogous to river migration across a flood plain in (a) cross sectional area and (b) plan in view.

700 5.3 Exploring potential controls on network patterns and variations in expression of MW_{Routes}

In this section, we explore spatial controls governing the overall pattern of the
subglacial hydrologic network, as well as variations in meltwater landform expression
705 (i.e. the balance between erosion / deposition and the resulting geomorphic



expression) along individual MW_{Routes} . Erosional and depositional features are frequently observed along the same MW_{Route} and even at the same location (e.g. eskers with lateral splay within wider meltwater channels (Fig. 4H)). This suggests that while spatial controls may be important and exert some control over the relative
710 'leakiness' of a conduit and therefore the resulting geomorphic signature at any location, there is also a temporal control. This is likely related to short-term variations in the magnitude and rate of subglacial meltwater delivery to the bed and the systems' ability to accommodate it.

715 We observe a high degree of channelisation across this sector of the ice sheet bed, but this is not uniform, with the densest areas of MW_{Routes} coinciding with the 'roughest' basal topography (Fig. 8). This may be the result of subglacial drainage route fragmentation around bed obstacles, with a greater number of tributaries and broken patterns common in regions of high bed roughness (e.g. Test Site 3). Basal
720 topography also preconditions the large-scale spatial structure of surface drainage (Ignéczi et al., 2018) and the association between rough areas and dense clusters of MW_{Routes} could be a response to more surface water penetrating to the bed as the result of extensive crevassing. In Greenland crevasses capture a significant amount of surface water – more than moulins or the hydrofracture of surface lakes (Kozioł et al., 2017). Surface meltwater inputs are thought to be an important control on the
725 distribution of drainage across the bed (e.g. Gulley et al., 2012; Banwell et al., 2016) and the formation and evolution of subglacial meltwater landforms (e.g. Banerjee and McDonald, 1975; St-Onge, 1984; Hooke and Fastook, 2007; Storrar et al., 2014b; Livingstone et al., 2015; Peterson and Johnson, 2017).

730

Qualitatively, there are markedly fewer MW_{Routes} coinciding with palaeo-ice stream locations – particularly the Dubawnt Lake Ice Stream (Fig. 9). In addition, the network pattern of MW_{Routes} corresponding with the location of the Dubawnt Lake Ice Stream are more dendritic and extend further towards the ice divide. These observations are
735 consistent with Livingstone et al., (2015), who find fewer eskers on palaeo-ice stream beds where modelled subglacial meltwater drainage is greatest. We suggest the scarcity of MW_{Routes} beneath palaeo-ice streams is due to lower ice-surface slopes and hydraulic gradients, which favour distributed rather than channelised drainage (e.g. Kamb, 1987; Bell, 2008). Where channelised drainage does occur beneath palaeo-ice



740 streams, network patterns are typically more dendritic, which may also be the result of shallower hydraulic gradients enabling greater lateral water flow.

Dynamic mass loss via streaming / surging has implications for ice sheet stability (e.g. Bell, 2008; Christianson et al., 2014; Christoffersen et al., 2014). The Keewatin
745 sector of the LIS exhibits a relatively low frequency of ice streams (Margold et al., 2015; Stokes et al., 2016). While this may be partially attributed to the resistant bed of the shield (Clayton et al., 1985; Kamb, 1987; Stokes and Clark, 2003a, b), we also suggest that efficient evacuation of meltwater through the dense channelised network that developed in this region during the final stages of deglaciation, as the climate
750 warmed (Storrar et al., 2014b), would have inhibited the development of fast flow and potentially contributed to the shut-down of existing ice streams (Lelandais et al., 2018). This is consistent with modern observations that link decadal-scale ice-flow decelerations with more pervasive and efficient drainage channelisation driven by increased surface meltwater inputs to the bed (Sole et al., 2013; Tedstone et al., 2014; van de Wal et al., 2015; Davison et al., 2019). We therefore hypothesise that this large-scale inverse relationship between drainage channelisation and ice streaming will exist in other palaeo-ice sheet settings. This potential drainage control on ice-sheet activity may also influence the pace of deglaciation; we note slower retreat rates (~ 230 m yr⁻¹) in the northwest of the study area, which coincide with the highest density of
755 MW_{Routes}, compared to much faster retreat rates (~ 540 m yr⁻¹) associated with the sparsest MW_{Routes}. This conclusion is tentative given uncertainty in the regions deglacial chronology (Dyke et al., 2003) and requires further testing.

At a large-scale, there is a general tendency for MW_{Routes} to form on till, which is
765 more easily eroded than bedrock and where geomorphic evidence is likely to be better developed. Eskers are over-represented on harder, more resistant rock (Fig. 7d) where R-channels are more likely to form (Clark and Walder, 1994; Storrar, 2014a), while there is a slight tendency for meltwater channels (i.e. incisional features) to form on the softer, more erodible sedimentary rock (Fig. 7b). Eskers with lateral splay (i.e. depositional features) appear preferentially on till blankets (Fig. 7c) where there is an
770 abundance of sediment that may overwhelm and clog up the conduit (Burke et al., 2015), while isolated esker ridges favour thin till and are under-represented on thick till. Though detailed long-profiles (Fig. 10) hint at local relationships between bed



775 substrate changes and the resultant landform expression, we caution against the
assumption that this is a widespread occurrence rather than an isolated coincidence.

5.4 Relevance for understanding Greenland's hydrology and associated ice dynamic variations

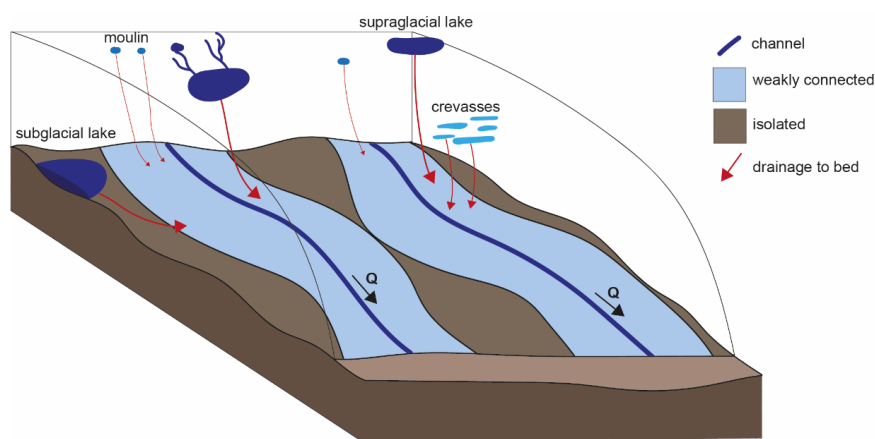
780 Western sectors of the contemporary Greenland Ice Sheet are analogous to our
study area: both are underlain by resistant Precambrian Shield rocks and both
experience(d) rapid retreat and high meltwater production rates. This is also similar to
southern Sweden, which lay beneath the palaeo Scandinavian Ice Sheet, where
similar geomorphic features to those described here, occur extensively (e.g. Peterson
785 et al., 2017; Peterson and Johnson, 2017). This study therefore has potential
implications for our understanding of the impact of subglacial hydrology on overlying
ice dynamics and ice flow regulation of past, current and future ice sheets.

790 The interaction between a subglacial conduit and the surrounding weakly-
connected drainage system (VPA) is believed to be widespread in contemporary
glaciological settings (e.g. Hubbard et al., 1995; Gordon et al., 1996; Bartholomaeus et
al., 2008; Werder et al., 2013; Tedstone et al., 2014) and has been identified as key
to understanding ice velocity variations and predicting future ice sheet mass loss
(Davison et al., 2019). However, the true extent and influence of VPAs beneath the
795 Greenland Ice Sheet is unknown due to the challenge of observing contemporary
subglacial environments. Palaeo-studies, such as this one, offer the potential to reveal
new insights into the nature and configuration of the subglacial hydrological system at
an ice sheet scale.

800 Based on our proposed model and the observations within this study we suggest
that the VPA is widespread across the Keewatin sector of the LIS, which may be
analogous to parts of western Greenland. The drainage footprint is considerably more
dense if we consider $MW_{\text{Corridors}}$ as well as esker ridges as indicators of areas of the
bed which were influenced by subglacial meltwater. The drainage footprint in our study
805 is estimated to cover ~13 % of the bed (using average width and spacing of MW_{Routes})
but could realistically vary between 5 % (lower quartile width and upper quartile
spacing) and 36 % (upper quartile width and lower quartile spacing) if we assume that



MW_{Routes} were active at the same time. This represents an area 25 times greater than that of eskers alone which cover ~0.5 % of the bed (using average esker width (100 m) and spacing (18.8 km; Storrar et al., 2014b). The dynamic influence is likely to extend even further beyond the VPA due to lateral stress transfer within the ice (Tedstone et al., 2014). In the longer term, increased channelisation may have additional ice dynamic implications; effectively removing large volumes of meltwater and reducing ice velocity, potentially limiting dynamic mass loss via streaming / surging (e.g. Storrar et al., 2014b).



820 **Figure 13.** Schematic of the VPA (light blue) beneath a contemporary ice sheet with inputs from the surface and the bed influencing discharge (Q) and therefore the VPA.

6. Conclusions

825

We identified and mapped all visible traces of subglacial meltwater drainage in the Keewatin sector of the former LIS. We found that wider meltwater features (meltwater tracks, meltwater channels and eskers with lateral splays on the order of 100s to 1000s m) flanking or joining up intervening segments of esker ridges were common. These have previously been termed and described as different features. However, owing to similarities in spacing, morphometry and spatial location (i.e. part of the same

830



integrated network), we propose collectively grouping these features under the term
MW_{Corridor} (table 2). Combining multiple features within a single MW_{Routes} map (i.e. esker
ridges and all varying geomorphic expressions of MW_{Corridors}), we have created the
835 first large-scale holistic map of subglacial meltwater drainage.

Based on our observations and modern analogues, we propose a new model
which accounts for the formation and geomorphic variations of MW_{Corridors}. In this
model, we propose that a central conduit (i.e. the esker) interacts with the surrounding
840 distributed drainage network or VPA (i.e. the MW_{Corridor}) with the relative extent /
intensity of this interaction, determined by the magnitude and rate of meltwater delivery
to the subglacial conduit and the resulting water pressure variability. Controls
governing the geomorphic expression of the VPA, such as net erosion or deposition,
is likely a combination of glaciological (i.e. relative water pressure fluctuation) and
845 background controls (i.e. topography, basal substrate). Eskers likely represent the
final depositional imprint of channelised drainage within the large-scale MW_{Routes}
network, with formation close to the ice margin, while the corridors represent a
composite imprint of drainage over a longer time period. If our model is correct,
incorporating the width of the VPA (i.e. the 'weakly connected' drainage system), the
850 drainage footprint in this sector of the ice sheet covered 5–36 % of the bed (on
average), which is 25 times greater than previously assumed from esker studies alone,
which only account for the central conduit.

Our results suggest that the overall distribution and pattern of drainage is
855 influenced by background topography, with greater relief resulting in denser
channelised networks, possibly due to fragmentation of subglacial drainage around
basal obstacles and / or enhanced meltwater delivery to the bed through crevasses.
Channelised drainage is relatively rare beneath palaeo ice streams, which may favour
distributed drainage configurations due to the lower ice surface slopes and hydraulic
860 gradients. Meltwater drainage may also influence ice dynamics, with the high degree
of channelisation observed in the region able to efficiently dewater the bed causing
ice-flow deceleration and limiting ice stream activity.

Further research should focus on determining how common this proposed
865 interaction between conduits and the surrounding distributed drainage system is



beneath other palaeo and contemporary ice sheets and the controls governing its variability. We hypothesise that where less surface meltwater is delivered to the bed or ice-surface slopes are shallower, for instance, when the LIS was larger and the climate colder, the geomorphic expression will be less extensive and fainter. This is
870 because conduits are less likely to evolve due to lower hydraulic gradients, and their interaction with the surrounding distributed system reduced because of invariant melt supply. Understanding where this interaction and signature occurs will help confirm or refute our proposed model, and develop understanding of how meltwater drainage evolves over long time-scales and influences ice dynamics and mass balance.

875

7. Acknowledgements

This work was funded through: “Adapting to the Challenges of a Changing
880 Environment” (ACCE); a NERC funded doctoral training partnership ACCE DTP (NE/L002450/1). This work also benefitted from the PALGLAC team of researchers who received funding from the European Research Council (ERC) under the European Union’s Horizon 2020 research and innovation programme (Grant agreement No. 787263). DEMs were provided by the Polar Geospatial centre under
885 NSF-OPP awards 1043681, 1559691, and 1542736.

8. References

- 890 Andrews, L.C. Catania, G.A. Hoffman, M.J. Gulley, J.D. Lüthi, M.P. Ryser, C. et al., Direct observations of evolving subglacial drainage beneath the Greenland Ice Sheet. *Nature*, 514(7520). 80–83. 2014
- Aylsworth, J. M. and Shilts, W. W. Glacial features around the Keewatin Ice Divide: Districts of
895 Mackenzie and Keewatin. Geological Survey of Canada, Map 24-1987. 1:1,000,000. 1989.
- Aylsworth, J.M. Shilts, W.W. Russel, H.A.J. Pyne, D.M. Eskers around the Keewatin Ice Divide: Northwest Territories and Nunavut. Geological Survey of Canada, Open File, 7047. 2012.
- 900 Banerjee, I. McDonald, B.C. Nature of esker sedimentation. In: Jopling, A.V. McDonald, B.C. (Eds.), *Glaciofluvial and Glaciolacustrine Sedimentation*, vol 23. Society of Economic Palaeontologists and Mineralogists. Special Publication. 304-20. 1975.



- 905 Banwell, A.D. Arnold, N.S. Willis, I.C. Tedesco, M. Ahlstrøm, A.P. Modelling supraglacial water routing and lake filling on the Greenland Ice Sheet. *J. Geophys. Res.* 117. 2012.
- 910 Banwell, A. Hewitt, I. Willis, I. Arnold, A. Moulin density controls drainage development beneath the Greenland ice sheet. *Journal of Geophysical Research: Earth Surface.* 121: 2248-69. 2016.
- 915 Bartholomaeus, T.C., Anderson, R.S. Anderson, S.P. Response of glacier basal motion to transient water storage. *Nature Geoscience*, 1. 33–37. 2008.
- 920 Bell, R.E. The role of subglacial water in ice-sheet mass balance. *Nat. Geosci.* 1(5): 297-304. 2008.
- 925 Bindschahler, R.A. The importance of pressurized subglacial water in separation and sliding at the glacier bed. *Journal of Glaciology.* 57: 929-41. 1983.
- 930 Bingham, R.G. Hubbard, A.L. Nienow, P.W. Sharp, M.J. An investigation into the mechanisms controlling seasonal speedup events at a High Arctic glacier. *Journal of Geophysical Research.* 113. 2008.
- 935 Bolduc, A.M. The formation of eskers based on their morphology, stratigraphy and lithologic composition, Labrador, Canada (Unpublished Ph.D thesis). Lehigh University. 1992.
- 940 Boulton, G. S., Caban, P. E. and Van Gijssel, K. Groundwater flow beneath ice sheets: part I - large scale patterns. *Quaternary Science Reviews*, 14, 545-562. 1995.
- 945 Boulton, G.S. Lunn, R. Vidstrand, P. Zatspein, S. Subglacial drainage by groundwater-channel coupling, and the origin of esker systems: Part I – Glaciological observations. *Quaternary Science Reviews.* 26(7–8). 1067-90. 2007a.
- 950 Boulton, G.S. Lunn, R. Vidstrand, P. Zatspein, S. Subglacial drainage by groundwater-channel coupling, and the origin of esker systems: Part II - Theory and simulation of a modern system. *Quaternary Science Reviews.* 26(7–8). 1091–105. 2007b.
- 955 Boulton, G. S., Hagdorn, M., Maillot, P. B. and Zatspein, S. Drainage beneath ice sheets: groundwater-channel coupling, and the origin of esker systems from former ice sheets. *Quaternary Science Reviews*, 28, 621-638. 2009.
- 960 Boulton, G.S. Hindmarsh, R.C.A. Sediment deformation beneath glaciers: rheology and geological consequences. *Journal of Geophysical Research.* 92. 9059-82. 1987.
- 965 Brennand, T.A. Deglacial meltwater drainage and glaciodynamics: Inferences from Laurentide eskers, Canada. *Geomorphology.* 32(3–4). 263–93. 2000.
- 970 Brennand, T.A. Shaw, J. Tunnel channels and associated landforms, south-central Ontario: their implication for ice-sheet hydrology. *Canadian Journal of Earth Sciences.* 31. 505-22. 1994.
- 975 Burke, M.J. Brennand, T.A. Perkins, A.J. Evolution of the subglacial hydrologic system beneath the rapidly decaying Cordilleran Ice Sheet by ice-dammed lake drainage: implications for meltwater-induced ice acceleration. *Quaternary Science Reviews.* 50: 125-40. 2012.



- 955 Burke, M.J. Brennand, T.A. Sjogren, D.B. The role of sediment supply in esker formation and ice tunnel evolution. *Quaternary Science Reviews*. 115: 50-77. 2015.
- 960 Carlson, A.E. Legrande, A.N. Oppo, D.W. Came, R.E. Schmidt, G.A. Anslow, F.S. Licciardi, J.M. Obbink, E.A. Rapid early Holocene deglaciation of the Laurentide ice sheet. *Nature Geoscience*. 1(9): 620-24. 2008.
- Carlson, A.E. Anslow, F.S. Obbink, E.A. LeGrande, A.N. Ullman, D.J. Licciardi, J.M. Surface melt driven Laurentide Ice Sheet retreat during the early Holocene. *Geophysical Research Letters*. 36. 2009.
- 965 Chandler, B. M. P., Lovell, H., Boston, C. M., Lukas, S., Barr, I. D., Benn, D. I., Clark, C. D., Darvill, C. M., Evans, D. J. A., Ewertowski, M., Loibl, D., Margold, M., Otto, J., Roberts, D. H., Stokes, C. R., Storrar, R. D. and Stroeven, A. Glacial geomorphological mapping: a review of approaches and frameworks for best practice. *Earth-Science Reviews*, 185, 806-846. 2018.
- 970 Christianson, K. Peters, L.W. Alley, R.B. Anandakrishnan, S. Jacobel, R.W. Riversman, K.W. Muto, A. Keisling, B.A. Dilatant till facilitates ice-stream flow in northeast Greenland. *Earth Planet. Sci. Lett.* 401: 57-69. 2014.
- 975 Christoffersen, P. Bougamont, M. Carter, S.P. Fricker, H.A. Tulaczyk, S. Significant groundwater contribution to Antarctic streams hydrologic budget. *Geophysical Research Letters*. 41. 2003-10. 2014.
- 980 Clark, P.U. Walder, J.S. Subglacial drainage, eskers, and deforming beds beneath the Laurentide and Eurasian ice sheets. *Geol. Soc. Am. Bull.* 106: 304 – 14. 1994.
- Clayton, L. Teller, J.T. Attig, J.W. Surging of the southwestern part of the Laurentide ice sheet. *Boreas*. 14: 235-41. 1985.
- 985 Cowton, T. Nienow, P. Sole, A. Wadham, J. Lis, G. Bartholomew, I. et al., Evolution of drainage system morphology at a land-terminating Greenlandic outlet glacier. *Journal of Geophysical Research. Earth Surface Processes*. 118. 29-41. 2013.
- 990 Cowton, T. Nienow, P. Bartholomew, I. Sole, A. Mair, D. Rapid erosion beneath the Greenland ice sheet. *Geology*. 40: 343:46. 2012.
- Cummings, D.I. Kjarsgaard, B.A. Russell, H.A.J. Sharpe, D.R. Eskers as mineral exploration tools. *Earth Science Reviews*. 109: 32-43. 2011a.
- 995 Cummings, D.I. Gorrell, G. Guillbault, J-P. Hunter, J.A. Logan, C. Ponomarenko, D. Pugin. A. J-M. Pullan, S.E. Russell, H.A.J. Sharpe, D.R. Sequence stratigraphy of a glaciated basin fill, with a focus on esker sedimentation. *Geological Society of American Bulletin*. 2011b.
- 1000 Cutler, P.M. Colgan, P.M. Mickelson, D.M. Sedimentological evidence for outburst floods from the Laurentide Ice Sheet margin in Wisconsin, USA: implications for tunnel-channel formation. *Quaternary International*. 90. 23-40. 2002.



- 1005 Das, S.B. Joughin, I. Behn, M.D. Howat, I.M. King, M.A. Lizarralde, D. Bhatia, M.P. Fracture propagation to the base of the Greenland Ice Sheet during supraglacial lake drainage. *Science*. 320 (5877). 963-64. 2008.
- 1010 Davison, B.J. Sole, A.J. Livingstone, S.J. Cowton, T.W. Nienow, P.W. The influence of hydrology on the dynamics of land-terminating sectors of the Greenland Ice Sheet. *Front. Earth Sci.* 7:10. 2019.
- Doyle, S.H. Hubbard, A. Fitzpatrick, A.A.W. van As, D. Mikkelsen, A.B. Pettersson, R. et al., Persistent flow acceleration within the interior of the Greenland ice sheet. *Geophysical Research Letters*. 41: 899-905. 2014.
- 1015 Doyle, S.H. Hubbard, A. Van De Wal, R.S. van As, D. Scharrer, K. Meierbachtol, T.W. et al., Amplified melt and flow of the Greenland ice sheet driven by late-summer cyclonic rainfall. *Nature Geoscience*. 8: 647-53. 2015.
- 1020 Dredge, L. Nixon, F. Richardson, R. Surficial Geology, Northwestern Manitoba: Geological Survey of Canada, 'A' Series Map 1608A, 1: 500 000. 1985.
- Dyke, A.S. Moore, A. Robertson, I. Deglaciation of North America. Geological Survey of Canada. Open File, 1574. 2003.
- 1025 Englehardt, H. Harrison, W. Kamb, B. Basal sliding and conditions at the glacier bed as revealed by bore-hole photography. *Journal of Glaciology*. 20: 469-508. 1978.
- 1030 Fitzpatrick, A.A. Hubbard, A. Joughin, I. Quincey, D.J. Van As, D. Mikkelsen, A.P. et al., Ice flow dynamics and surface meltwater flux at a land-terminating sector of the Greenland ice sheet. *Journal of Glaciology*. 59: 687-96. 2013.
- Fowler, A. Sliding with cavity formation. *Journal of Glaciology*. 33: 131-41. 1987.
- 1035 Fulton, R.J. Surficial materials of Canada. Geological Survey of Canada, 'A' Series Map 1880A. 1:5,000,000. 1995.
- 1040 Gordon, S. Sharp, M. Hubbard, B. Smart, C. Ketterling, B. Willis, I. Seasonal reorganization of subglacial drainage inferred from measurements in boreholes. *Hydrological Processes*. 12. 105-33. 1998.
- Gorrell, G. Shaw, J. Deposition in an esker, bead and fan complex, Lanark, Ontario, Canada. *Sedimentary Geology*. 72(3-4): 285-314. 1991.
- 1045 Greenwood, S.L. Clark, C.D. The sensitivity of subglacial bedform size and distribution to substrate lithological control. *Sedimentary Geology*. 232: 130-44. 2010.
- 1050 Glasser, N.F. Sambrook Smith, G.H. Glacial meltwater erosion of the Mid-Cheshire Ridge: implications for ice dynamics during the Late Devensian glaciation of northwest England. *Journal of Quaternary Science*. 14: 703-10. 1999.
- Gudmundsson, G.H. Transmission of basal variability to a glacier surface. *Journal of Geophysical Research: Solid Earth*. 108(B5). 2003.



- 1055 Gulley, J.D. Grabiec, M. Martin, J.B. Jania, J. Catania, G. Glowacki, P. The effect of discrete recharge by moulins and heterogeneity in flow-path efficiency at glacier beds on subglacial hydrology. *Journal of Glaciology*. 58(211). 2012.
- 1060 Hebrand, M. Amark, M. Esker formation and glacier dynamics in eastern Skane and adjacent areas, southern Sweden. *Boreas*. 18(1): 67-81. 1989.
- Hewitt, I.J. Modelling distributed and channelized subglacial drainage: the spacing of channels. *Journal of Glaciology*. 57(202). 2011.
- 1065 Hewitt, I.H. Creyts, T.T. A model for the formation of eskers. *Geophysical Research Letters*. 46. 2019.
- Hodge, S.M. Direct measurements of basal water pressures: progress and problems. *Journal of Glaciology*. 23, 309-19. 1979.
- 1070 Hoffman, M.J. Andrews, L.C. Price, S.A. Catania, G.A. Neumann, T.A. Luthi, M.P. et al., Greenland subglacial drainage evolution regulated by weakly connected regions of the bed. *Nature Communications*. 7: 13903. 2016.
- 1075 Hooke, R.L. Fastook, J. Thermal conditions at the bed of the Laurentide ice sheet during deglaciation: implications for esker formation. *Journal of Glaciology*. 53(183). 2006.
- Hooke, R.L. Jennings, C.E. On the formation of the tunnel valleys of the southern Laurentide ice sheet. *Quaternary Science Reviews*. 25(11–12). 1364–72. 2006.
- 1080 Hooke, R. LeB. Laumann, T. Kohler, J. Subglacial water pressures and the shape of subglacial conduits. *Journal of Glaciology*. 36 (122). 67-71. 1990.
- 1085 Hoyal, D.C.J.D. Van Wagoner, J.C. Adair, N.L. Deffenbaugh, M. Li, D. Sun, T. Huh, C. Griffin, D.E. Sedimentation from jets: A depositional model for clastic deposits of all scales and environments: Salt Lake City, Utah, Search and Discovery Article No. 40082, American Association of Petroleum Geologists Annual Meeting, May 14, 2003, 10.
- 1090 Hubbard, B.P. Sharp, M.J. Willis, I.C. Nielsen, M.K. Smart, C.C. Borehole water-level variation and the structure of the subglacial hydrological system of Haut Glacier d'Arolla, Valais, Switzerland. *Journal of Glaciology*. 41(139). 572–83. 1995.
- 1095 Ignéczi, A. Sole, A.J. Livingstone, S.J. Ng, F.S.L. Yang, K. Greenland ice sheet surface topography and drainage structure controlled by transfer of basal variability. *Frontiers in Earth Science*. 6: 101. 2018.
- Iken, A. Bindschadler, R.A. Combined measurements of subglacial water pressure and surface velocity of Findelengletscher, Switzerland: conclusions about drainage system and sliding mechanisms. *Journal of Glaciology*. 32: 101-19. 1986.
- 1100 Iken, A. Rothlisberger, H. Flotron, A. Harberli, W. The uplift of Unteraargletscher at the beginning of the melt season – a consequence of water storage at the bed? *Journal of Glaciology*. 29: 28-47. 1983.



- 1105 Iverson, N.R. Baker, R.W. Hooke, R.L. Hanson, B. Jansson, P. Coupling between a glacier and a soft bed: I. A relation between effective pressure and local shear stress determined from till elasticity. *Journal of Glaciology*. 45: 31-40. 1999.
- 1110 Jørgensen, F. Sandersen, P.B.E. Buried and open tunnel valleys in Denmark – erosion beneath multiple ice sheets. *Quaternary Science Reviews*. 25(11-12): 1339-63. 2006.
- 1115 Joughin, I. Das, S.B. King, M. Smith, B.E. Howat, I.M. Moon, T. Seasonal speedup along the western flank of the Greenland Ice Sheet. *Science*. 320: 781-83. 2008.
- 1120 Kamb, B. Glacier surge mechanism based on linked cavity configuration of the basal water conduit system. *Journal of Geophysical Research, Solid Earth*. 92(B9). 9038-100. 1987.
- 1125 Kamb, B. Raymond, C. Harrison, W. Engelhardt, H. Echelmeyer, K. Humphrey, N. et al., Glacier surge mechanism: 1982-1983 surge of Variegated Glacier, Alaska. *Science*. 227: 469-79. 1985.
- 1130 Kehew, A.E. Nicks, L.P. Straw, W.T. Palimpsest tunnel valleys: evidence for relative timing of advances in an interlobate area of the Laurentide ice sheet. *Ann. Glaciol.* 28: 47 – 52. 1999.
- 1135 Kehew, A.E., Piotrowski, J.A. and Jørgensen, F. Tunnel valleys: Concepts and controversies - A review. *Earth-Science Reviews*. 113(1–2). 33–58. 2012.
- 1140 Kleman, J. Borgström, I. Reconstruction of palaeo-ice sheets: the use of geomorphological data. *Earth Surface Processes and Landforms*. 21(10): 893-909. 1996.
- 1145 Koziol, C. Arbold, A. Pope, A. Colgan, W. Unifying supraglacial meltwater pathways in the Paakitsoq region, West Greenland. *Journal of Glaciology*. 63(239): 464-76. 2017.
- 1150 Kerr, D. Knight, R. Sharpe, D. Cummings, D. Reconnaissance surficial geology, Lynx Lake, Northwest Territories, NTS 75-J: Geological Survey of Canada, 1: 125 000. 2014a.
- 1155 Kerr, D. Knight, R. Sharpe, D. Cummings, D. Reconnaissance surficial geology, Walmsley Lake, Northwest Territories, NTS 75-N, Canadian Geoscience Map-140: Geological Survey of Canada, 1:125 000. 2014b.
- 1160 Lee, H.A. Craig, B.G. Fyles, J.G. Keewatin ice divide. *Geol. Soc. Am. Bull.* 68: 1760-61. 1957.
- 1165 Lelandais, T. Ravier, E. Pochat, S. Bourgeois, O. Clark, C. Mourgues, R. Strzeczynski, P. Modelled subglacial floods and tunnel valleys control the life cycle of transitory ice streams. *The Cryosphere*. 12: 2759-72. 2018.
- 1170 Lewington, E.L.M. Livingstone, S. Sole, A.J. Clark, C.D. Ng, F. An automated method for mapping geomorphological expressions of former subglacial meltwater pathways (hummock corridors) from high resolution digital elevation data. *Geomorphology*. 339: 70-86. 2019.



- Livingstone, S.J. and Clark, C.D. Morphological properties of tunnel valleys of the southern sector of the Laurentide ice sheet and implications for their formation. *Earth Surface Dynamics*. 4. 567–89. 2016.
- 1155 Livingstone, S.J. Storrar, R.D. Hillier, J.K. Stokes, C.R. Tarasov, L. An ice-sheet scale comparison of eskers with modelled subglacial drainage routes. *Geomorphology*. 246. 104–12. 2015.
- Livingstone, S.J. Lewington, E.L.M. Clark, C.D. Storrar, R.D. Sole, A.J. McMartin, I. Dewald, N. Ng, F.. A quasi-annual record of time-transgressive esker formation: implications for ice sheet reconstruction and subglacial hydrology. *The Cryosphere Discuss.* In review, 2019.
- 1160
- Lliboutry, L. General theory of subglacial cavitation and sliding of temperate glaciers. *Journal of Glaciology*. 7. 21-58. 1968.
- 1165 Mäkinen, J. Time-transgressive deposits of repeated depositional sequences within interlobate glaciofluvial (esker) sediments in Köyliö, SW Finland. *Sedimentology* 50. (2): 337-60. 2003.
- Mäkinen, J. Kajutti, K. Palmu, J-P. Ojala, A. Ahokangas, E. Triangular-shaped landforms reveal subglacial drainage routes in SW Finland. *Quaternary Science Reviews*. 164. 37–53. 2017.
- 1170
- Margold, M. Stokes, C.R. Clark, C.D. Ice streams in the Laurentide Ice Sheet: Identification, characteristics and comparison to modern ice sheets. *Earth Science Reviews*. 143. 117-46. 2015.
- 1175 Margold, M. Stokes, C.R. Clark, C.D. Reconciling records of ice streaming and ice margin retreat to produce a palaeographic reconstruction of the deglaciation of the Laurentide Ice Sheet. *Quaternary Science Reviews*. 189: 1-30. 2018.
- McMartin, I. Henderson, P. J. Evidence from Keewatin (central Nunavut) for paleo-ice divide migration. *Géographie physique et Quaternaire*, 58, 163-186. 2004.
- 1180
- Mooers, H.D. On the formation of the tunnel valleys of the Superior Lobe, Central Minnesota. *Quaternary Research*. 32: 24 – 35. 1989.
- 1185 Ng, F. Ignéczi, A. Sole, A.J. Livingstone, S.J. Response of surface topography to basal variability along glacial flowlines. *Journal of Geophysical Research: Earth Surface*. 123: 2319-40. 2018.
- Nienow, P. Sharp, M. Willis, I. Seasonal changes in the morphology of the subglacial drainage system, Haut Glacier d’Arolla, Switzerland. *Earth Surface Processes and Landforms*. 23: 825-84. 1998.
- 1190
- Noh, M.J. Howat, I.M. Automated stereo-photogrammetric DEM generation at high latitudes: Surface Extraction with TIN-based Search-space Minimisation (SETSM) validation and demonstration over glaciated regions. *GISci. Remote Sens.* 52(2), 198-217. 2015.
- 1195
- Nye, J. Water at the bed of a glacier. *IASH Publications* 95. (Symposium at Cambridge 1969 – Hydrology of Glaciers). Pp. 189-194. 1973.
- 1200 Ó Cofaigh, C. Tunnel valley genesis. *Progress in Physical Geography*. 20. 1-19. 1996.



- 1205 Ojala, A.E.K. Peterson, G. Mäkinen, J. Johnson, M.D. Kajutti, K. Palmu, J-P. Ahokangas, E. Öhrling, C. Ice-sheet scale distribution and morphometry of triangular shaped hummocks (murtoos): a subglacial landform produced during rapid retreat of the Scandinavian Ice Sheet. *Anal. of Glaciology*. 1-12. 2019.
- Palmer, S. Shepherd, A. Nienow, P. Joughin, I. Seasonal speed-up of the Greenland ice sheet linked to routing of surface water. *Earth Planet Science Letters*. 302: 423-28. 2011.
- 1210 Perkins, A.J., Brennand, T.A. Burke, M.J. Towards a morphogenetic classification of eskers: Implications for modelling ice sheet hydrology. *Quaternary Science Reviews*. 134. 19–38. 2016.
- 1215 Peterson, G. Johnson, M.D. Hummock corridors in the south-central sector of the Fennoscandian ice sheet, morphometry and pattern. *Earth Surface Processes and Landforms*. 43: 919-29. 2018.
- 1220 Peterson, G. Johnson, M.D. Smith, C.A. Glacial geomorphology of the south swedish uplands – focus on the spatial distribution of hummock tracts. *Journal of Maps*. 13(2): 534 – 44. 2017.
- Peterson, G. Johnson, M.D. Dahlgren, S. Pässe, T. Alexanderson, H. Genesis of hummocks found in tunnel valleys: an example from Horda, southern Sweden. *GFF*. 140(2): 189 – 544. 2018.
- 1225 Piotrowski, J.A. Tunnel-valley formation in north west Germany – geology, mechanisms of formation and subglacial bed conditions for the Bornhöved tunnel valley. *Sedimentary Geology*. 89. 107-41. 1994.
- 1230 Piotrowski, J.A. Channelized subglacial drainage under soft-bedded ice sheets: evidence from small N-channels in Central European lowland. *Geol. Q.* 43(2): 153-62. 1999.
- Porter, C., Morin, P., Howat, I., Noh, M.J., Bates, B., Peterman, K., Keeseey, S., Schlenk, M., Gardiner, J., Tomko, K. Willis, M., et al., ArcticDEM. *Harvard Dataverse*, V1. 2018.
- 1235 Powell, R.D. Glacimarine processes at grounding-line fans and their growth to ice-contact deltas. *Geological Society, London, Special Publications*, 53(1): 53-73. 1990.
- 1240 Praeg, D. Seismic imaging of mid-Pleistocene tunnel valleys in the North Sea Basin – high resolution from low frequencies. *Journal of Applied Geophysics*. 53 273-298. 2003.
- Prowse, N.D. Morphology and Sedimentology of Eskers in the Lac de Gras Area, Northwest Territories, Canada. PhD Thesis. Carleton University. Ottawa, Canada. 2017.
- 1245 Price, S.F. Payne, A.J. Catania, G.A. Neumann, T.A. Seasonal acceleration of inland ice via longitudinal coupling to marginal ice. *Journal of Glaciology*. 54: 213-19. 2008.
- Punkari, M. Glacial and glaciofluvial deposits in the interlobate areas of the Scandinavian Ice Sheet. *Quaternary Science Reviews*, 16, 741-753. 1997.



- 1250 Rampton, V.N. Large-scale effects of subglacial meltwater flow in the southern Slave Province, Northwest Territories, Canada. *Canadian Journal of Earth Sciences*. 37(1). 81–93. 2000.
- Rothlisberger, H. Water pressure in Intra- and Subglacial Channels. *Journal of Glaciology*. 11: 177–203. 1972.
- 1255 Russell, A.J., Gregory, A.R., Large, A.R., Fleisher, P.J. and Harris, T.D. Tunnel channel formation during the November 1996 jökulhlaup, Skeiðarárjökull, Iceland. *Annals of Glaciology*, 45, 95–103. 2007.
- 1260 Russell, A.J. Roberts, M.J. Fay, H. Marren, P.M. Cassidy, N.J. Tweed, F.S. Harris, T. Icelandic jökulhlaups impacts: Implications for ice-sheet hydrology, sediment transfer and geomorphology. *Geomorphology*. 75: 33–64. 2006.
- 1265 Rust, B.R. Romanelli, R. Late quaternary subaqueous outwash deposits near Ottawa, Canada. A.V. Jopling, B.C. McDonald (Eds.), *Glaciofluvial and Glaciolacustrine Sedimentation*, Soc. Econ. Paleontol. Mineral., Spec. Publ. 177–92. 1975.
- Sergienko, O. V. Glaciological twins: Basally controlled subglacial and supraglacial lakes. *Journal of Glaciology*. 59(213). 3–8. 2013.
- 1270 Sharpe, D., Kjarsgaard, B. Knight, R.D. Russell, H.A.J. Kerr, D.E. Glacial dispersal and flow history, East Arm area of Great Slave Lake, NWT, Canada. *Quaternary Science Review*. 165: 49 – 72. 2017.
- 1275 Shepherd, A. Hubbard, A. Nienow, P. King, M. McMillan, M. Joughin, I. Greenland ice sheet motion coupled with daily melting in late summer. *Geophysical Research Letters*. 36: 2–5. 2009.
- Shilts, W.W. Aylsworth, J.M. Kaszycki, C.A. Klasson, R.A. Canadian Shield. In: Graf, W.L. (Ed.), *Geomorphological Systems of North America*. Geological Society of America, Boulder, Colorado. pp. 119–61. Centennial Special Volume 2. 1987.
- 1280 Shreve, R.L. Movement of water in glaciers. *Journal of Glaciology*. 11(62). 205–14. 1972.
- Shreve, R.L. Esker characteristics in terms of glacial physics, Katahdin esker system, Maine. *Geol. Soc. Am. Bull.* 96, 639 – 46. 1985.
- 1285 Sissons, J.B. A subglacial drainage system by the Tinto Hills, Lancashire. *Trans Edinb. Geol. Soc.* 18: 175 – 92. 1961.
- 1290 Sjogren, D.B. Fisher, T.G. Taylor, L.D. Jol, H.M. Munro-Stasiuk, M.J. Incipient tunnel channels. *Quaternary International*. 90. 41–56. 2002.
- Smith, M.J. Clark, C.D. Methods for the visualisation of digital elevation models for landform mapping. *Earth Surface Processes and Landforms*. 30(7) : 885–900. 2005.
- 1295 Sole, A. Nienow, P. Bartholomew, I. Mair, D. Cowton, T. Tedstone, A. et al., Winter motion mediates dynamic response of the Greenland Ice Sheet to warmer summers. *Geophysical Research Letters*. 40(15). 3940–44. 2013.



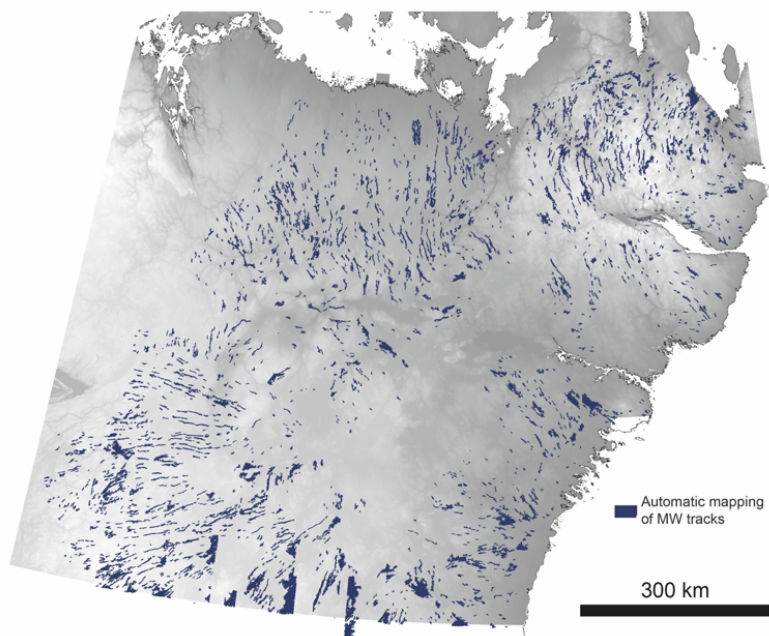
- 1300 Stevens, L.A. Behn, M.D. Das, S.B. Joughin, I. Noel, B.P. Broeke, M.R. et al., Greenland Ice Sheet flow response to runoff variability. *Geophys. Res. Lett.* 43: 11295-303. 2016.
- Stokes, C.R. Clark, C.D. The Dubawnt Lake palaeo-ice stream: evidence for dynamic ice sheet behaviour on the Canadian Shield and insights regarding the controls on ice-stream location and vigour. *Boreas.* 32(1): 263-79. 2003a.
- 1305 Stokes, C.R. Clark, C.D. Laurentide ice streaming on the Canadian Shield: A conflict with the soft-bedded ice stream paradigm? *Geology.* 31(4): 347-50. 2003b.
- 1310 Stokes, C. R., Margold, M., Clark, C. D. Tarasov, L. Ice stream activity scaled to ice sheet volume during Laurentide Ice Sheet deglaciation. *Nature*, 530: 322-326. 2016.
- St-Onge, D.A. Surficial deposits of the Redrock Lake area, District of Mackenzie; in *Current Research, Part A, Geological Survey of Canada, Paper 84 (1A).* 271-78. 1984.
- 1315 Storrar, R.D. Reconstructing subglacial meltwater dynamics from the spatial and temporal variation in the form and pattern of eskers. Doctoral thesis, Durham University. 2014.
- 1320 Storrar, R. D., Ewertowski, M., Tomczyk, A., Barr, I. D., Livingstone, S. J., Ruffell, A., Stoker, B. Evans, D. J. A. Equifinality and preservation potential of complex eskers. *Boreas.* 2019.
- Storrar, R.D. Livingstone, S.J. Glacial geomorphology of the northern Kivalliq region, Nunavut, Canada, with an emphasis on meltwater drainage systems. *J. Maps.* 13: 153-64. 2017.
- 1325 Storrar, R.D. Stokes, C.R. Evans, D.J.A. A map of large Canadian eskers from Landsat imagery. *Journal of Maps.* 3: 456-73. 2013.
- Storrar, R.D. Stokes, C.R. Evans, D.J.A. Morphometry and pattern of a large sample (> 20,000) of Canadian eskers and implications for subglacial drainage beneath ice sheets. *Quaternary Science Reviews.* 105: 1 – 25. 2014a.
- 1330 Storrar, R.D., Stokes, C.R. Evans, D.J.A. Increased channelization of subglacial drainage during deglaciation of the Laurentide Ice Sheet. *Geology.* 42(3). 239–42. 2014b.
- 1335 Stroeven, A. P., Hättestrand, C., Kleman, J., Heyman, J., Fabel, D., Fredin, O., Goodfellow, B. W., Harbor, J. M., Jansen, J. D., Olsen, L., Caffee, M. W., Fink, D., Lundqvist, J., Rosqvist, G. C., Strömberg, B. Jansson, K. N. Deglaciation of Fennoscandia. *Quaternary Science Reviews*, 147, 91-121. 2016.
- 1340 Tedstone, A.J. Nienow, P.W. Gourmelen, N. Dehecq, A. Goldberg, D. Hanna, E. Decadal slowdown of a land-terminating sector of the Greenland Ice Sheet despite warming. *Nature.* 526: 692 – 95. 2015.
- 1345 Tedstone, A.J. Nienow, P.W. Gourmelen, N. Sole, A.J. Greenland ice sheet annual motion insensitive to spatial variations in subglacial hydraulic structure. *Geophysical Research Letters.* 41: 8910-17. 2014.
- Tedstone, A.J. Nienow, P.W. Sole, A.J. Mair, D.W. Cowton, T.R. Bartholomew, I.D. et al., Greenland ice sheet motion insensitive to exceptional meltwater forcing. *Proceedings of*



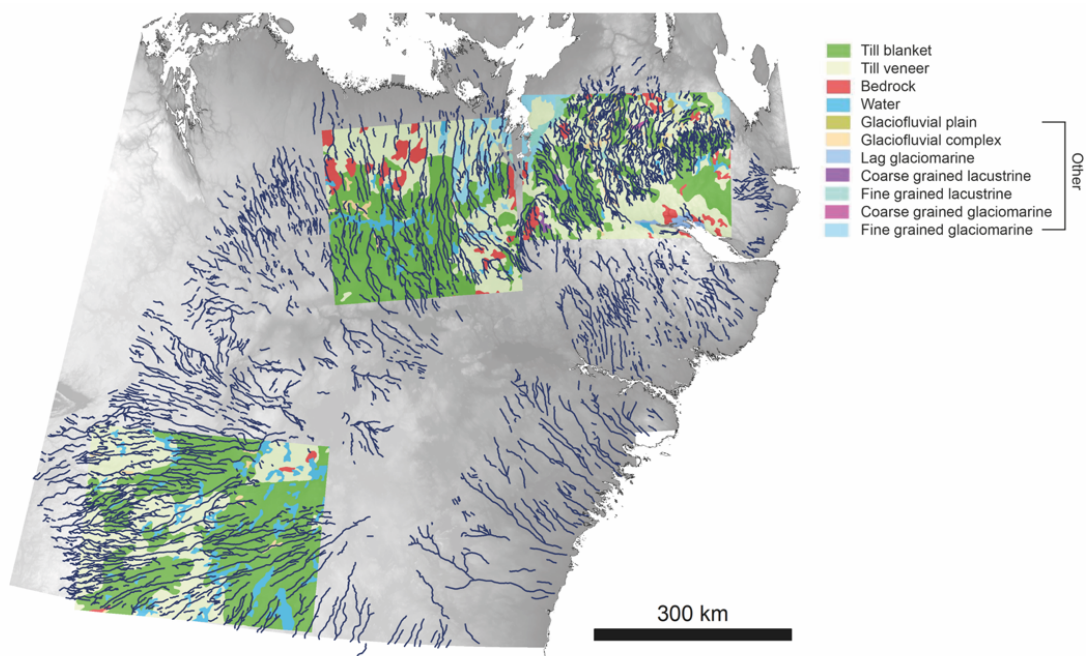
- 1350 the National Academy of Sciences of the United States of America. 110(49). 19719–24. 2013.
- Utting, D.J., Ward, B.C. Little, E.C. Genesis of hummocks in glaciofluvial corridors near the Keewatin Ice Divide, Canada. *Boreas*. 38(3). 471–481. 2009.
- 1355 Van der Vegt, P., Janszen, A. Moscariello, A. Tunnel valleys: current knowledge and future perspectives. Geological Society, London, Special Publications. 368(1). 75–97. 2012.
- 1360 van de Wal, R.S.W. Boot, W. Van den Broeke, M.R. Smeets, C.J.P.P. Reijmer, C.H. Donker, J.J.A. et al., Large and rapid melt-induced velocity changes in the ablation zone of the Greenland Ice Sheet. *Science*. 321. 111-13. 2008.
- 1365 van de Wal, R.S.W. Smeets, C.J.P.P. Boot, W. Stoffelen, M. van Kampen, R. Doyle, S.H. et al., Self-regulation of ice flow varies across the ablation area in south-west Greenland. *Cryosphere*. 9: 603-11. 2015.
- Walder, J.S. Hydraulics of subglacial cavities. *Journal of Glaciology*. 32(112). 439-445. 1986.
- 1370 Walder, J.S. Fowler, A. Channelized subglacial drainage over a deformable bed. *Journal of Glaciology*. 40(134). 1994.
- Ward, B.C. Dredge, L.A. Kerr, D.E. Surficial geology, Lac de Gras, District of Mackenzie, Northwest Territories (NTS 76-D): Geological Survey of Canada, 1:125 000. 1997.
- 1375 Warren, W.P. Ashley, G.M. Origins of the ice-contact stratified ridges (eskers) of Ireland. *Journal of Sedimentary Research*. 64(3a). 433-49. 1994.
- Weertman, J. General theory of water flow at the base of a glacier or ice sheet. *Reviews of Geophysics and Space Physics*. 10. 287-333. 1972.
- 1380 Werder, M.A. Hewitt, I.J. Schoof, C.G. Flowers, G.E. Modeling channelized and distributed subglacial drainage in two dimensions. *Journal of Geophysical Research: Earth Surface*. 118(4). 2140–58. 2013.
- 1385 Wheeler, J.O. Hoffman, P.F. Card, K.D. Davidson, A. Sanford, B.V. Okulitch, A.V. Roest, W.R. Geological Map of Canada. Geological Survey of Canada, map 1860A. 1996.
- 1390 Zwally, H.J. Abdalati, W. Herring, T. Larson, K. Saba, J. Steffen, K. Surface melt induced acceleration of the Greenland Ice Sheet flow. *Science*. 297. 218-22. 2002.
- 1395



9. Appendices



1400 **Figure A1.** Automatic mapping output (cleaned up) for test site using code associated with Lewington et al., 2019.



1405 **Figure A2.** Surface substrate across the three test sites (left – right) used for analysis in section 3.3

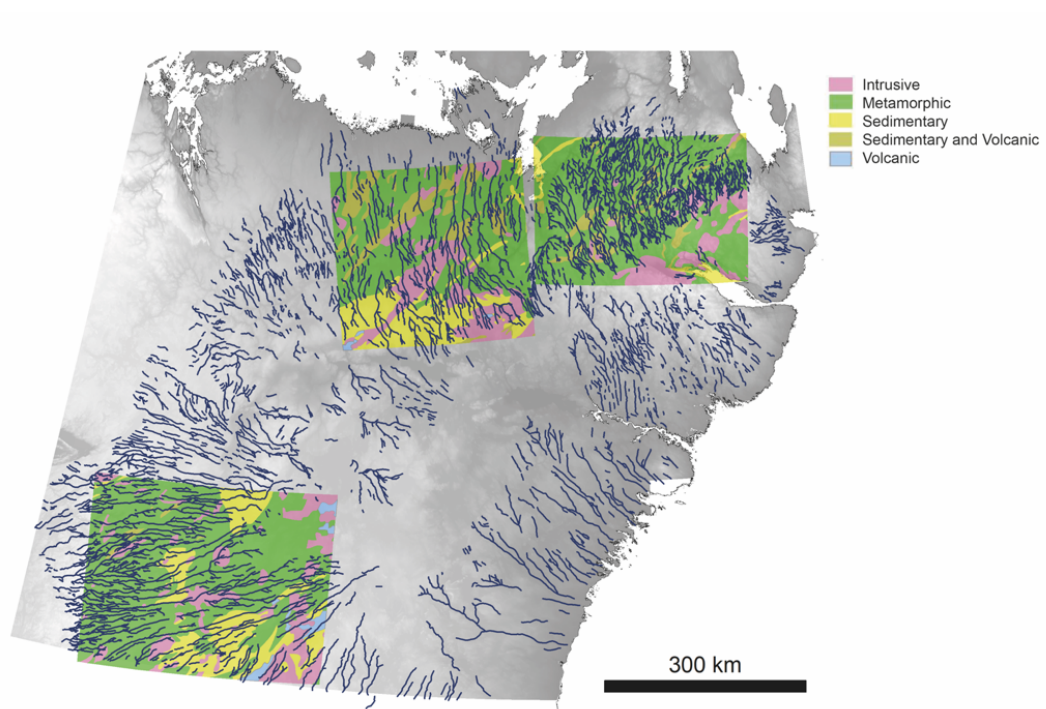


Figure A3. Bed geology across the three test sites (left to right) used for analysis in section 3.3